

4-23-2009

# Design of Arterial Blood Pressure, Heart Rate Variability, and Breathing Rate Monitoring Device

Mastan Singh Kalsi  
*McMaster University*

---

## Recommended Citation

Singh Kalsi, Mastan, "Design of Arterial Blood Pressure, Heart Rate Variability, and Breathing Rate Monitoring Device" (2009). *EE 4BI6 Electrical Engineering Biomedical Capstones*. Paper 7.  
<http://digitalcommons.mcmaster.ca/ee4bi6/7>

This Capstone is brought to you for free and open access by the Department of Electrical and Computer Engineering at DigitalCommons@McMaster. It has been accepted for inclusion in EE 4BI6 Electrical Engineering Biomedical Capstones by an authorized administrator of DigitalCommons@McMaster. For more information, please contact [scom@mcmaster.ca](mailto:scom@mcmaster.ca).

Design of Arterial Blood Pressure, Heart Rate Variability,  
and Breathing Rate Monitoring Device

by

Mastan Singh Kalsi

Electrical and Biomedical Engineering Design Project (4BI6)  
Department of Electrical and Computer Engineering  
McMaster University  
Hamilton, Ontario, Canada

Design of Arterial Blood Pressure, Heart Rate Variability,  
and Breathing Rate Monitoring Device

by

Mastan Singh Kalsi

Department of Electrical and Computer Engineering  
Faculty Advisor: Prof. Doyle

Electrical and Biomedical Engineering Project Report  
Submitted in partial fulfillment of the requirements  
for the degree of bachelor of Engineering

McMaster University  
Hamilton, Ontario, Canada  
April 23, 2009

Copyright © March 2009 by Mastan Singh Kalsi

## **ABSTRACT**

An infrared emitter and a photodiode pressed against a highly vascular surface of a finger or on the brachial artery allow the photodiode to generate a current based on the infrared light it receives. Moreover, the varying amount of blood in the artery as the pulse passes through it impacts the light intensity the photodiode receives. Therefore, the signal received from the photodiode can be used to calculate the instantaneous heart rate and consequently the heart rate variability. Furthermore, the signal received from the photodiode is the photoplethysmographic (PPG) waveform which can be used to calculate the pulse transit time (PTT), the pulse height, and the breathing rate. PTT is the time interval between a peak on the finger PPG waveform and the corresponding peak on the brachial artery PPG waveform. Since PTT is inversely related to blood pressure changes, and the pulse height is proportional to the difference between the systolic and the diastolic pressure in the arteries, with correlation coefficients calculated with the aid of a standard blood pressure monitoring system, arterial blood pressure values can be calculated. By comparing the theories encompassing the hardware design with the experimental results the report articulates the effectiveness of the device.

**Keywords** – arterial blood pressure, brachial artery, breathing rate, heart rate variability, photodiode, photoplethysmographic, PPG, PTT, pulse height, systolic and diastolic pressure

## **ACKNOWLEDGEMENTS**

Mastan Singh Kalsi, the author of this report, with sincere appreciation would like to thank many individuals who have contributed greatly in providing knowledge, support, and encouragement throughout this project.

Yousuf Jawahar, Omer Waseem, and Aiyush Bansal, the members of the NIHMS project and the author's colleagues, provided tremendous assistance in the successful completion of this project. They also acted as test subjects during numerous stages of testing and troubleshooting.

Dr. Doyle, the supervisor and co-coordinator of this project, has been a great teacher and mentor. The NIHMS team would also like to thank Dr. Hubert deBruin for his great words of encouragement and wisdom and letting the team borrow a sphygmomanometer for calibration purposes.

The author further wishes to express appreciation to and thank his parents, family, and friends for their wealth of knowledge on this project. The author would like to recognize and thank the editor of this report, and a great friend, Akhil Chandan.

## TABLE OF CONTENTS

Abstract .....	ii
Acknowledgements.....	iii
Table of Contents .....	iv
LIST OF TABLES .....	vi
List of figures .....	vii
Nomenclature .....	viii
1 Introduction.....	1
1.1 Objectives .....	1
1.2 Scope and Methodology .....	2
2 Literature Review.....	3
2.1 Blood Pressure from Blood Flow .....	3
2.2 Breathing Rate .....	3
2.3 Photoplethysmography (PPG) .....	4
3 Problem Statement and Methodology of Solution.....	6
3.2 Theory of measuring Blood Pressure using PPG Pulse Height .....	7
3.3 Theory of measuring Blood Pressure using Pulse Transit Time.....	7
3.3 Problem Statement .....	9
3.4 Methodology of Solution .....	10
3.4.1 Calculating Systolic and Diastolic Blood Pressure.....	10
3.4.2 Calculating Breathing Rate .....	12
3.4.3 Calculating Heart Rate Variability.....	12
4 Design Procedures .....	13
4.1 Selection of Material .....	13
4.2 <i>IR Emitter Diode Circuit</i> .....	14
4.3 Photodiode Signal to an Electrical Voltage Signal .....	14
4.4 Initial Amplification.....	15
4.5 Noise Removal.....	16
4.6.1 Active Signal Filtering.....	18
4.7 Passive Signal Filtering.....	20
4.8 Summing Amplifier .....	21
4.9 Final Amplification.....	22
4.9.1 Measuring the Pulse Height and Pulse Transit Time.....	22
4.9.2 Measuring the Breathing Rate .....	23
4.10 Breathing Rate Envelope Detection using Hardware .....	24
4.11 Breathing Rate Envelope Detection using Software.....	25
4.12 Complete Hardware Circuit .....	27
5 Results and Discussion .....	28
5.1 Testing.....	28
5.2 Hardware Results .....	30
5.3 Signal Transmission from Hardware to Computer .....	33
5.4 Digital Filtering.....	33
5.5 Peak Detection Algorithm.....	35

5.6	Arterial Blood Pressure Calculation Using Pulse Height .....	37
5.7	Arterial Blood Pressure Calculation Using Pulse Transit Time .....	38
5.8.	<i>Heart Rate Variability Data Processing</i> .....	40
5.9	Instantaneous Breathing Rate Calculation .....	41
6	Conclusions.....	42
7	Recommendations.....	43
8	Appendix A: Hardware Designs .....	44
9	Appendix B: Data processing in matlab .....	50
9.1	Breathing Rate Envelop Detection.....	50
9.2	Peak Detection Algorithm Implementation and the remaining Calculations .....	50
10	References.....	53
11	Vitae.....	55

## LIST OF TABLES

Table 1 - Major Parts used in the Hardware Circuits.....	13
Table 2 - Time Constant Determination Chart .....	24
Table 3 - Physiological Data obtained from the Sphygmomanometer .....	33
Table 4 - Test Values obtained for Calibration.....	37
Table 5 - Calibration Factors for to determine SBP and DBP .....	37
Table 6 - Blood Pressure Calculations using the Pulse Height Correlation Coefficients .....	38
Table 7 - Correlation Coefficients for Pulse Transit Time .....	39
Table 8 - Instantaneous Blood Pressure Calculations for two peaks using PTT .....	39



## LIST OF FIGURES

Figure 1 - Major strata of the reflected light intensity at the PPG site .....	5
Figure 2 - A period of PPG showing the anacrotic and the catacrotic phase, dicrotic notch, as well as the PPG peak height.....	6
Figure 3 - Cardiovascular network showing the path from the aorta to the brachial artery [9].....	8
Figure 4 - Pulse transit time using two PPG waveforms [ 7]. .....	11
Figure 5 - Emitter Diode Circuit.....	14
Figure 6 - Current to voltage conversion circuit.....	15
Figure 7 – Pre-amplification inverting amplifier.....	16
Figure 8 - Active Band Pass Filter Circuit.....	19
Figure 9 - Magnitude transfer function for the active band pass filter .....	20
Figure 10 - Passive band pass filter .....	21
Figure 11 - Summing Amplifier .....	22
Figure 12 - Non-inverting amplifier circuit .....	23
Figure 13 - Final amplification block for the breathing rate calculation .....	24
Figure 14 - Envelope Detection Circuit.....	25
Figure 15 - Front end of the flashlight transducer .....	29
Figure 16 - Finger PPG waveform observed on the oscilloscope.....	31
Figure 17 - Brachial PPG (top), Finger PPG (bottom) .....	32
Figure 18 - Raw PPG signals as sent to the computer.....	34
Figure 19 - Digital filtered finger PPG (blue) along with the brachial PPG (green) .....	35
Figure 20 - Three points compared in the peak detection algorithm .....	35
Figure 21- Peak amplitudes to determine peak height.....	37
Figure 22 - SBP and DBP values calculated for the labeled peaks .....	38
Figure 23 - Stability of the correlation coefficients tested over the course of 12 peaks.....	39
Figure 24 - Stability of PTT correlation coefficients observed through 12 consecutive SBP readings.....	40
Figure 25 - HRV calculated using standard deviation and a set of IHR values.....	40
Figure 26 – Breathing Rate Measurement and envelope detection .....	41
Figure 27 - First PPG Transducer .....	44
Figure 28 - Device Hardware Complete Circuit Block .....	45
Figure 29 - An Improved Transducer .....	46
Figure 30 - Device Hardware Prototype with the Transducer .....	47
Figure 31 - Hardware Prototype for Breathing Rate Envelope Detection .....	48
Figure 32 - Site for Brachial PPG Detection .....	49

## **NOMENCLATURE**

Arterial Blood Pressure: Pressure of the blood in the arterial system.

Heart Rate Variability: The rate at which the heart rate varies with the heart rate measured at the arteries.

Breathing Rate: The rate of breathing as measured from the photoplethysmographic waveform of the arterial system in the finger.

Non-invasive: Such that an object or material do not cut through the skin or cause an alternation in anything beneath the skin.

NIHMS: Non-invasive Health Monitoring System

## 1 INTRODUCTION

The need for a device that continuously monitors the health of an individual arises when the person interested in monitoring desires to be informed of the health status as soon as a critical condition is observed so the appropriate remedy can be immediately provided. There are many applications of this device. A parent may want to monitor the health of a child with a cardiac disorder, or a doctor may need to study how a patient's health condition varies in a period of few days. While a single blood pressure (BP) or heart rate (HR) reading is interesting, it is sometimes more important to assess the health status based on trends in the BP and HR readings. A BP reading decreasing in a short period of time would suggest that the patient is going into shock. A long term trend of BP values maybe requested to assess if the patient is experiencing hypertension. Hypertension is a major risk factor of myocardial infarction, congestive heart failure, stroke, kidney failure and blindness. More than 15% of Canadians suffer from high blood pressure [1]. The existing BP devices are mainly cuff based that are bulky, inconvenient to carry, and do not allow for BP value to be obtained in a beat-by-beat manner. Therefore, a cuff-less and non-invasive device is desirable that allows continuous BP measurements to be made.

While there has been an increased demand of a continuous health monitoring system the importance of remotely monitoring the physiological condition of a soldier and firefighter has gained significant momentum. Breathing rate is one of the first vital signs examined following an injury. Sudden changes in breathing rate can be due to airway obstruction, wounds to the abdomen or pleural cavity, or blunt chest trauma [2]. Furthermore, since heart rate variability (HRV) indicates autonomic nervous system activity its readings report detrimental physiological changes [3]. Thus, an HRV reading can provide an advanced warning of critical conditions to allow for faster medical attention using a wireless transmission of the health status.

### *1.1 Objectives*

The objective of this project was to design and develop a device, named Non-invasive Health Monitoring System (NIHMS), that picks up physiological signals from the body and transmits them to a data processing unit for meaningful results to be computed and displayed. The detection of the signal from the body has to be safe and non-invasive. The transducer needs to be

designed such that it does not inject any current into the patient. While the focus of this module of the project is on measuring arterial blood pressure (ABP), heart rate and breathing rate, NIHMS has the capacity to integrate multiple transducers detecting several physiological signals simultaneously. The physiological signals measured in collaboration with the NIHMS team include ABP, heart rate, breathing rate, blood oxygen saturation, body temperature and the resting potential of the retina using electrooculography (EOG).

Once the signal is detected it needs to be converted to the form that can be transmitted using a wireless device. The wireless transmission of the signal is crucial because the party interested in observing the data maybe far away. The device needs to be able to integrate with a network at the university, hospital or another workplace.

### *1.2 Scope and Methodology*

This module, referred to as the project from this point, focuses on measuring arterial blood pressure, heart rate variability and breathing rate. The physiological signal measured from the body is converted to a sufficiently scaled voltage reading. This signal is then sent to a microprocessor to be passed to a Bluetooth module. The signal then gets transmitted to a data processing unit, that can be any computer or a smartphone equipped with Bluetooth technology. The microprocessor and the Bluetooth hardware and software was designed and developed by the NIHMS team member, Omer Waseem. Hence, this report will not discuss the details of these two components except for the conditions it places on the signal it receives. The microprocessor requires that the signal passed to it must be in the positive Volts range. To meet this requirement, a summing amplifier was integrated into the project hardware circuit. This matter is further discussed in the latter sections of the report.

Data processing was done in software to reduce the cost of the project and to limit the hardware circuitry to avoid making the device bulky. The software chosen for this project was MATLAB version 7.5. Data processing further cleans the signal for an accurate prognosis. Signal processing techniques such as fast Fourier transform (FFT) were used in the cleaning of the signal. While much of the noise was filtered in the hardware, some instrumentation noise was

unavoidable due to the monetary budget constraints on this project. Data processing was also used to compute the heart rate variability and the breathing rate values.

## **2 LITERATURE REVIEW**

Blood pressure is the pressure that the blood exerts on the walls of the vessels that the blood travels within. In general, blood pressure being referred to is the systemic arterial blood pressure, which is the pressure in the arteries of the body. The ABP is used to push the blood through the arteries and into the tissue. The supply of blood to a region is called perfusion. Blood pressure is needed to allow for tissue perfusion. When the heart ventricles contract, expelling the blood from the heart, blood pressure is generated and it is at its maximum in the arterial system. This is called the systolic blood pressure (SBP) during the period when the heart is contracting. When the heart is relaxing and the ventricles are refilling with the blood returning from the body, the pressure in the arteries is very low. This lower reading is called the diastolic blood pressure (DBP). It is important to note that for a healthy individual the blood pressure is well maintained. As the heart contracts and the blood enters the arteries the pressure widens the arteries. The elasticity properties of the arteries allow them to recoil as the heart relaxes and the pressure drops. The recoiling effect pushes the blood further maintaining the DBP [4].

### *2.1 Blood Pressure from Blood Flow*

Blood pressure is mathematically calculated as the cardiac output times the peripheral resistance. The cardiac output is the product of heart rate and stroke volume. Cardiac output then is the volume of blood ejected by the heart per minute. As the cardiac output increases, the amount of blood entering the arteries increases. This increase in flow rate increases the blood pressure [4].

### *2.2 Breathing Rate*

As studied above, pressure travels down its gradient. The intake of air requires the pressure in the container to be lower than the atmospheric pressure. Thus, to allow inspiration the respiration muscles increase the volume of the thoracic cavity. According to Boyle's gas law, the increase in volume causes the pressure in the lungs to become lower than the atmospheric pressure. This in

turn lets the air enter the lungs. Likewise, the volume decrease of the thoracic cavity increases the pressure in the lungs allowing for expiration to take place.

It is important to note that since the volume of the entire thoracic cavity changes due to inspiration and expiration, the heart's blood inflow and outflow also get affected. This is simply because the heart resides in the thoracic cavity. Therefore, breathing in causes a slight decrease in pressure in the four chambers of the heart. This lowered pressure in the heart creates a larger pressure gradient with respect to the rest of the body resulting in an increased amount of blood return to the right side of the heart.

Since the right side of the heart gets the blood from the body, the larger pressure gradient allows for the higher cardiac input. However, the vessels that feed into the left side of the heart are the pulmonary veins. These veins reside in the thorax and experience the same pressure that the rest of the thoracic cavity does. As there is no increase in the pressure gradient for these veins the cardiac input to the left side of the heart remains unchanged [4].

### *2.3 Photoplethysmography (PPG)*

Photoplethysmography is a technique that uses a light emitter and detector to measure pulsatile blood flow. A diode is a device that has two electrodes and only allows current to flow in one direction. A light emitting diode (LED) is a P-N junction device that emits light when it is forward-biased. While the regular incandescent bulbs emit light over a large range of bandwidth, an LED emits light of a specific wavelength. In PPG, a corresponding photo-detector diode with the matching wavelength as the LED is used. The photo-detector diode is a semiconductor light sensor that generates a current proportional to the light intensity it receives [5].

If the light emitter and detector are placed on a highly vascular surface of a finger, the detector will pick up the light intensity reflected back from the tissue. There are many factors that affect the light after it is sent from the emitter and before it gets reflected to the detector. The blood volume and the surrounding tissue such as the blood vessel wall have the largest impact on the light that gets reflected. The reflected light intensity decreases as the blood volume increases in

the region where the diodes are placed. Therefore, as the blood volume varies according to the cardiac output, the reflected light intensity respectively gets affected. The result is an alternating current (AC) component of the PPG waveform. There is also a direct current (DC) component in the PPG waveform. This latter component is due to the tissues and the average amount of blood volume that always remain in the section of the artery being sampled. The figure below is a demonstration that shows the AC component riding on the DC signal. It can be observed that the reflected light due to the pulsatile arterial blood flow is much smaller than the DC component.

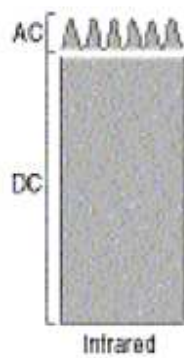


**Figure 1 - Major strata of the reflected light intensity at the PPG site**

### 3 PROBLEM STATEMENT AND METHODOLOGY OF SOLUTION

A clear definition of the problem statement, the solution and theories encompassing the hardware design are presented in this section.

#### 3.1 Decomposition Analysis of PPG

The Photoplethysmography technique used to study pulsatile arterial flow presents interesting useful subcomponents of the cardiac cycle. The right ventricle pumps the blood to the pulmonary circulation through the pulmonary arteries. The blood releases carbon dioxide and picks up oxygen through gas exchange in the alveoli of the lungs. The oxygenated blood then enters the left atrium through the pulmonary veins. The blood passes through a valve into the left ventricle, which then ejects the blood through the aorta and into the arteries. The deoxygenated blood returns from the body and enters the right atrium through the veins [4]. The contraction of the ventricles is called systole and the relaxation period when the ventricles are refilling is called diastole. A period of the PPG waveform can be split into two phases. The first rising edge is the anacrotic phase. This is the systolic upstroke time. The second falling edge is catacrotic phase characterized by the diastole. A dicrotic notch is also observed in the catacrotic phase. This notch is due to the sudden closing of the aortic valve resulting in retrograde flow and a subsequent temporary increase of blood volume in the arteries [5]. These main segments of the PPG along with the peak height are shown in the figure below.

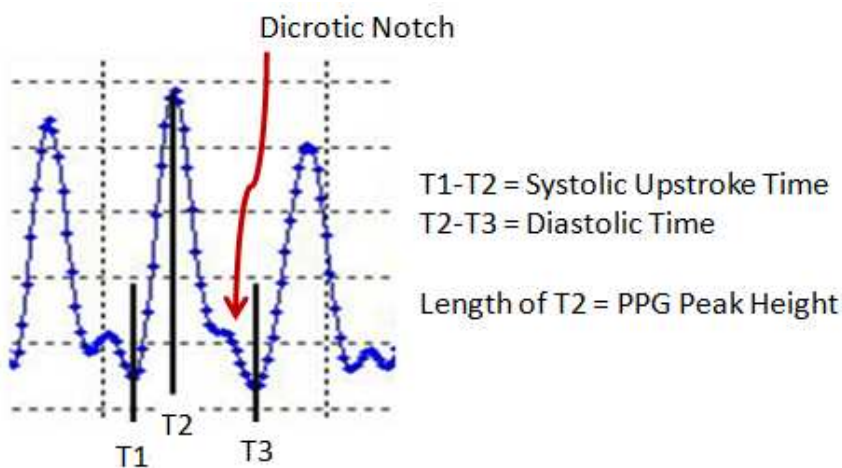


Figure 2 - A period of PPG showing the anacrotic and the catacrotic phase, dicrotic notch, as well as the PPG peak height.



### *3.2 Theory of measuring Blood Pressure using PPG Pulse Height*

From the above PPG decomposition analysis, the peak height is the difference between the maximum of a cardiac cycle and the previous minimum. This is the height of the pulsatile (AC) component of the PPG. It is proportional to the difference between the arterial systolic and diastolic pressures. However, this approach to measuring the blood pressure is not self sufficient because the SBP and the DBP values cannot be calculated from the pulse height alone without knowing a baseline blood pressure. Either the SBP or the DBP needs to be measured using another approach to extract any useful information from the pulse height.

Calibration requirements of this technique necessitate the need to consider the alternative approach of using the PPG pulse wave velocity.

### *3.3 Theory of measuring Blood Pressure using Pulse Transit Time*

The second technique also provides beat-to-beat tracking of the blood pressure. In this approach instead of the amplitude of the PPG waveform, the time variable was considered. The periodicity and the continuous flow of the PPG waveform allows for a beat-to-beat analysis along several interesting points on a peak.

Blood pressure is a function of cardiac output, which is the amount of blood volume output per cycle. It was noted earlier that an increase in the flow rate of the blood causes the blood pressure to rise. Thus, there exists a linear relationship between the blood pressure value and the rate at which the blood travels in the arteries. This flow rate can be calculated if the pulse wave velocity is known. Although, the PPG waveform is the technique used to measure blood flow in the arteries, the factor that relates the flow to the blood pressure is the pulse transit time (PTT). Determining the PTT is a difficult procedure.

Pulse transit time is the time interval for the arterial pulse pressure wave to travel from the aortic valve where it is ejected from the left ventricle to a peripheral site. This peripheral site can be anywhere along the brachial artery where the pulse can be felt the most. The brachial artery is the major blood vessel of the upper arm, so for this reason it is the artery that gets occluded when measuring blood pressure using the traditional mercury sphygmomanometer. The cardiovascular flow showing the blood flow from the aorta to the brachial artery is presented in the image below.

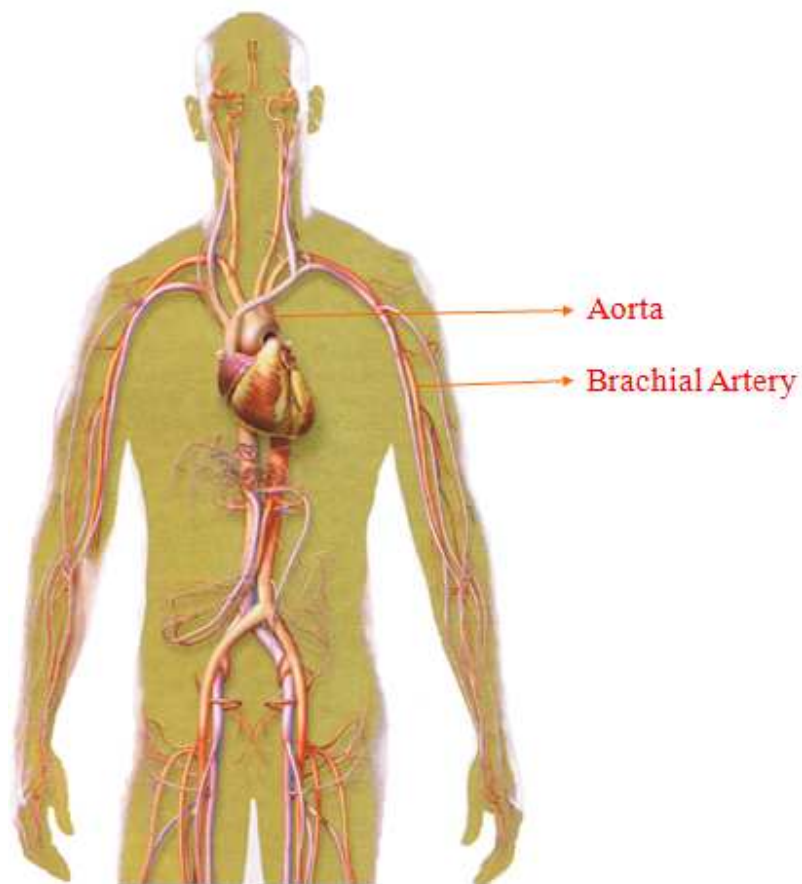


**Figure 3 - Cardiovascular network showing the path from the aorta to the brachial artery [9].**

To determine the time at which the blood leaves the aortic valve an electrocardiogram (ECG) is used. The QRS peak in the ECG waveform is a result of the ventricular contraction. Since, the R value in the QRS peak is highest amplitude, it is used as the marker for the time when the blood leaves the aortic valve. From this R peak value obtained, the PTT can be calculated.

The pulse transit time is calculated from the R peak in the ECG waveform to the foot of the PPG wave at the peripheral site. To calculate the blood pressure using the PTT, it is important to note the two quantities are related by an inverse relationship. This is because an increase in blood pressure results in an increase in blood velocity which means the blood reaches the peripheral site from the aortic valve in a smaller time interval. Consequently, a decrease in the blood pressure corresponds to a longer pulse transit time.

### *3.3 Problem Statement*

Although, direct measurements of blood pressure can be made using an invasive technique, a non-invasive and less cumbersome approach is preferred. In the past, the correlation between the pulse transit time and the arterial blood pressure is used to calculate the systolic and diastolic blood pressure values. However, this technique requires the use of an ECG, that makes the device bulky and unportable.

The problem is to design and develop an arterial blood pressure, heart rate variability, and breathing rate monitoring device without using an ECG. The device must be non-invasive and safe for the user to use. The device cannot be bulky and must not use the traditional cuff used in the past to measure blood pressure. The device must output a positive voltage signal that can be sent to the microprocessor. While software techniques can be used to filter instrumentation noise and to clean the signal, much of the filtering must take place in the hardware circuitry. The

power requirements of the device are also limited. Since a 9 Volt battery is easily accessible and safe to use, the preferred source voltage allowed for the hardware circuit is 9 Volts.

The device must provide a signal that can be used to calculate systolic and diastolic blood pressure reading within reasonable error. Majority of the project component for measuring blood pressure must be done in hardware. A transducer must be built that can be used on any individual. The transducer must also be non-invasive and safe to use. Since the heart rate variability and the breathing rate calculation are the minor components of the project, these measurements can be done in software alone.

The budget allowed for the project is a maximum of \$50 Canadian dollars. The completion timeline of the project is seven months.

### *3.4 Methodology of Solution*

#### 3.4.1 Calculating Systolic and Diastolic Blood Pressure

The problem statement requires that the ECG may not be used. The theory of using the PPG peak height requires some calculations that must be made. Therefore, a solution was found that combines the aforementioned theories involving the peak height and the pulse transit time.

The pressure waves travel along the arterial walls and therefore propagate slower under low blood pressure and faster under higher blood pressure. Thus, if the ECG in the pulse transit time calculation is replaced by another PPG signal then this approach provides additional information. If a PPG waveform is taken at a site along the brachial artery near the end of the upper arm and another PPG waveform is taken at the tip of the finger on the same side of the body, then the travel time for the PPG pulse from one site to the other can be classified as the pulse transit time. These two sites are clearly shown in the figure 4 below.

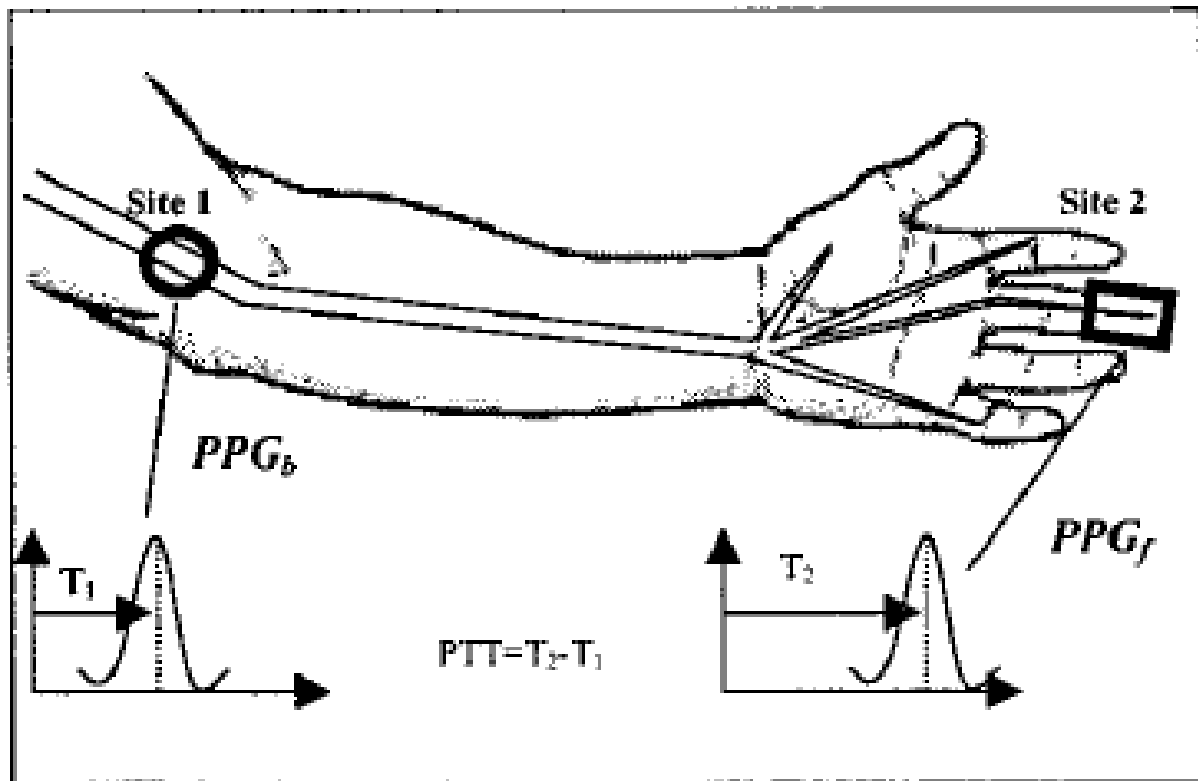


Figure 4 - Pulse transit time using two PPG waveforms [ 7].

Since the distance between the two sites can easily be measured, then by using the distance and the pulse transit time, pulse wave velocity (PWV) can be calculated. PWV is the velocity of the PPG waveform. Under high blood pressure the wave velocity propagates faster than under low pressures.

The pulse wave velocity also does not provide a mechanism to compute both the systolic and the diastolic blood pressure readings. However, with the aid of a traditional sphygmomanometer a correlation coefficient can be found between the pulse wave velocity and the systolic blood pressure reading. The correlation coefficient can be further used to allow the device to automatically calculate the subsequent systolic blood pressure readings.

Knowing the SBP readings, the DBP values can be calculated using the PPG peak height theory. Since the peak height corresponds to the difference in SBP and DBP, DBP value is a simple product calculation once the peak height is determined.

### 3.4.2 Calculating Breathing Rate

As discussed in the literary review, inhaling air results in an increased amount of blood returned to the heart due to the larger pressure gradient. Consequently, a larger volume of blood is also ejected that corresponds to an increased cardiac output value. Since the cardiac output is directly proportional to the blood pressure, the BP value also gets affected [4].

Respiration causes small variations in the peripheral circulation. These low frequency respiratory induced intensity variations provide a mechanism to measure the breathing rate using the PPG waveform [5].

### 3.4.3 Calculating Heart Rate Variability

Since a peak-to-peak blood flow is characterized by the PPG waveform, instantaneous heart rate (IHR) can be calculated per beat. Heart rate variability is calculated using the correlation between a set of instantaneous heart rate values. Standard deviation is used to compute the heart rate variability. In the equation below, N is the number of IHR values being considered,  $\mu$  is the average of the IHR values, and  $x_i$  is the each IHR.

$$S_N = \sqrt{\frac{1}{N} \sum_{i=1}^N (x_i - \mu)^2}$$

Equation 1 – Standard deviation used to calculate HRV

## 4 DESIGN PROCEDURES

This section details the hardware and software designs used to implement the methodologies described in the previous section. Specifically, major circuit components' characteristics are discussed, followed by the process of converting the light intensity variations caused by the changing blood flow into a voltage signal. Then detailed circuit analysis is presented for the rest of the hardware followed by the software algorithms.

### 4.1 Selection of Material

The infrared (IR) emitter and detector used in this project had a peak wavelength of 850 nm. Since the purpose of the photo-emitter and detector in this project is simply to measure the variation in the light intensity due to the changes in blood volume the exact peak wavelength of the pair is irrelevant as long as the blood volume changes can be measured. For this experiment, a typical peak wavelength between 600 nm to 900 nm is chosen in pulse oximetry, and because an emitter and detector pair with a peak wavelength of 850 nm is readily available, it is used in this project for the finger PPG.

**Table 1 - Major Parts used in the Hardware Circuits**

Part	Details		Cost/Unit (CDN)
<b>IR Emitting Diode<sup>1</sup></b>	Part Number:	TSHG6400	\$1.06
	Peak Wavelength:	850 nm	
	Forward Voltage:	$I_F = 100 \text{ mA}; V_F = 1.5 \text{ V}$	
		$I_F = 1 \text{ A}; V_F = 2.3 \text{ V}$	
<b>IR Photodiode<sup>2</sup></b>	Part Number:	SFH 203 P	\$0.72
	Peak Wavelength:	850 nm	
	Forward Voltage:	$I_F = 80 \text{ mA}; V_F = 1.3 \text{ V}$	
<b>IC OPAMP<sup>3</sup></b>	VCC = $\pm 16$ or 32		\$1.95

<sup>1</sup> <http://www.vishay.com/docs/84636/tshg6400.pdf>

<sup>2</sup> <http://parts.digikey.com/1/parts/1540920-photodiode-t1-3-4-sfh-203-p.html>

<sup>3</sup> <http://www.fairchildsemi.com/ds/LM/LM224.pdf>

#### 4.2 IR Emitter Diode Circuit

The following circuit is used to generate the light source that is transmitted to the artery through the skin. Unlike the photo diode, the emitter relies on the annihilation of electrons and holes through recombination. In this process, as the hole and an electron recombine, energy in the form of a photon is released equal to the bandgap of the semiconductor. For this emitter, the wavelength of the emitted photons is 850 nm.

The forward voltage of the emitter is 1.5 Volts, thus a 5 k $\Omega$  is used to reduce the current entering the emitter. Since the emitter used does not generate visible light, a webcam is used to test if the emitter is turned on. Furthermore, the input voltage is chosen to be 4.5 Volts to make it convenient to attain this input voltage from a conventional 9 Volt battery.

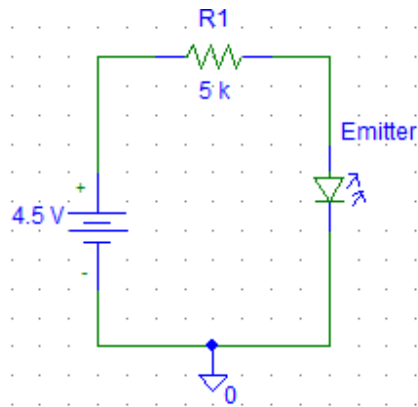


**Figure 5 - Emitter Diode Circuit**

#### 4.3 Photodiode Signal to an Electrical Voltage Signal

A fraction of the light emitted gets lost as a result of scattering, and another fraction gets lost in transmittance through the skin. Since the photo diode and the emitter are placed next to one another on the same side of the tissue, the photo diode picks up the reflected light. The reflectance of light is caused by the pulsatile blood flow and the surrounding tissue. This reflected light illuminates the depletion region of the pn junction diode then the photons are able to provide sufficient energy to cause the electrons to jump the semiconductor bandgap. This effect creates electron hole pairs.



The additional current created by the photon absorption can be modeled by a current source in parallel with the diode. This current is represented with the variable  $I$  in Figure 6, below.

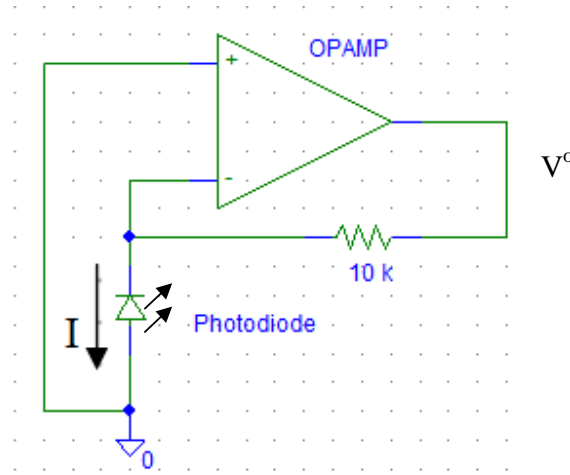


**Figure 6 - Current to voltage conversion circuit**

After the optical signal is converted to current, by using a resistor this signal gets converted to an electrical voltage signal. The current flows through the resistor producing an output voltage signal with the following relation for this circuit topology.

$$I = \frac{V^o - V^-}{10 \text{ k}\Omega}, \quad V^+ = V^- = 0, \quad \text{Output voltage} = I * 10 \text{ k}\Omega$$

**Equation 2 – Current to voltage conversion**

Therefore, this circuit block provides a gain of 10,000 V/V. The photon generated current in the nano Amperes range gets translated into a micro Volts range. While the signal in this form can be used to measure the PPG waveform, any sufficient filtering would almost completely attenuate the signal. A preamplifier can be used to increase the amplitude of the signal to a desired range.

#### *4.4 Initial Amplification*

The signal received from the previous block has a DC component as well as an AC from the pulsatile blood flow. The AC component of the signal is very small in comparison at this stage.

Since, the signal of interest is this alternating current component, the signal must be amplified before being filtered to remove the DC offset.

To accomplish the necessary amplification, an inverting amplifier is built at this stage. The positive input of this operation amplifier is grounded and a feedback network is formed using a 1 k $\Omega$  and a 1 M $\Omega$  resistor. Using Kirchoff's current law set of two port parameters are determined that characterize the complete amplifier block. The voltage gain of the inverting amplifier is negative. This indicates that the input pulsatile (sinusoidal) signal incurs a 180 degree phase shift. The amplifier circuit block is presented in Figure 7 below along with the Voltage gain equation.

$$\frac{\text{Input Signal}}{1 \text{ k}\Omega} = - \frac{\text{Output Signal}}{1 \text{ M}\Omega}$$

**Equation 3 – Voltage gain of an inverting amplifier using the two port parameters**

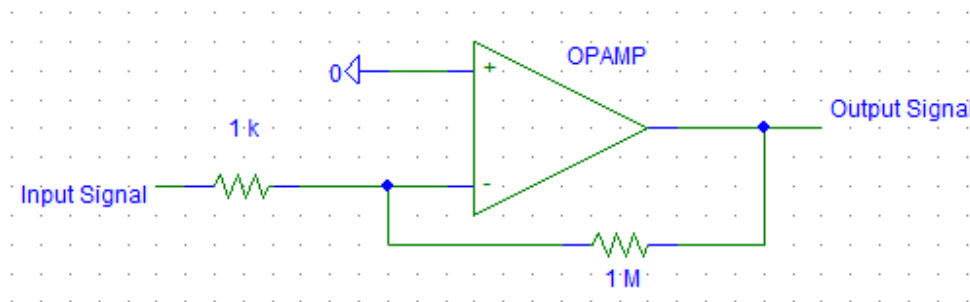


**Figure 7 – Pre-amplification inverting amplifier**

The absolute gain attained from this circuit block is 1000 times. Thus, the input signal in the micro-Volts range is amplified to a milli-Volts range.

#### 4.5 Noise Removal

The previous stage ensures that the signal is in a range such that it can be filtered to remove noise and extract the signal of interest. The purpose of this stage is to remove artifacts and undesired frequencies, avoid saturation, and increase the signal to noise ratio (SNR). Noise can arise from an external source such as the 60 Hz power-line or due to internal artifacts in the signal caused by motion and tremor through unavoidable movements.

Artifacts in a signal often occur due to interference, which is the imposition of the unwanted signal on the signal of interest. While the low frequency respiratory induced intensity variations in the photo diode signal are of primary interest in determining the breathing rate, it is a source of noise in the PPG waveform used to calculate pulse transit time.

The DC offset in the photo diode optical signal contains no useful information for any calculation and therefore needs to be attenuated to the maximum. This attenuation can be made possibly by considering the differences in the way the DC and the AC signal are being generated. The DC offset arises due to the reflectance of light from the tissue surrounding the pulsatile blood flow, and the significant property of this tissue is that it does not change in any shape or form in a small period of time. Then assuming that the DC offset will always be non-changing, it can be removed by passing the signal through a high pass filter. Since the DC offset has no frequency components above 0 Hz, any cut-off above this value for the high pass filter should attenuate the DC signal. However, because the filters do not cut off frequency components sharply the roll off property requires that the cut off frequency be slightly above the desired cut off value.

Another major source of noise in the signal was originating from the ambient noise. Although, the photo diode has a peak wavelength of 850 nm, it does take in photons with slightly different energy levels. The lighting in the room was being picked up by photo diode as the optical signal that distorts the PPG waveform. This was observed after passing the voltage signal through a high pass filter. While the filtering removed the DC offset, the AC signal was extremely noisy. The zoom function on the oscilloscope allowed the identification of a 60 Hz sinusoidal signal embedded in the PPG waveform. This noise was removed from the spectrum by suppressing all frequency components above 40 Hz. This task can be accomplished through the use of a low pass filter with a cut off frequency significantly lower than the 50-60 Hz ambient noise.

Motion artifact is another main source of noise. Since complete immobility of the arm or finger where the PPG transducer is placed is not realistic, some correction to remove this artifact needs to be implemented in the hardware circuitry. Although, the interference due to this nondeterministic noise can have large amplitudes, its frequency range is below 10 Hz [10].

Therefore, to reduce the impact of motion artifact on the PPG waveform a cut-off for the high pass filter must be below 10 Hz. However, to determine the exact cut-off frequency the signal of interest needs further analysis.

The removal of the DC offset and the ambient noise require in combination a band pass filter. The band pass filter can be realized by combining the characteristics of the low-pass and high-pass filters. Revising the signal of interest is helpful in designing the cut-off frequencies of the band pass filter. The PPG signal is essentially a beat-to-beat blood flow waveform varying according to the cardiac output and the heart rate. The slight variations in the cardiac output are of interest in calculating the breathing rate. However, the heart rate is the major characterizing aspect of the PPG waveform. A typical heart rate of 60 beats per minute (bpm) corresponds to 1 Hz. According to the Heart and Stroke Foundation, a normal heart rate is around 60 to 80 bpm<sup>4</sup>. Thus, a lower cut-off of 30 bpm corresponding to 0.5 Hz for the band pass filter should pass the signal of interest while attenuating the 0 Hz DC offset. Similarly, the upper cut-off frequency can be selected by suppressing any signal above 3.5 Hz (210 bpm). This cut-off will ensure the removal of any interference from the ambient noise and much of the motion artifact.

In determining the cut-off frequencies for the filter excessive bandwidth is avoided as it allows passage of voltage signals that tend to obscure the bioelectric signal of interest.

#### *4.6.1 Active Signal Filtering*

A filter is a circuit that is used to attenuate the undesired frequency components causing interference. Active filters make use of amplifiers in addition to the passive components such as resistors and capacitors, in order to obtain better performance than offered by the passive filters. Analog filters are based on the mathematical operator of differentiation. The DC component in the signal is removed by the derivative operator. In this respect, the gain increases linearly with frequency. Thus, higher frequencies receive linearly increasing gain that results in the attenuation of the 0 Hz.

---

<sup>4</sup> [http://www.heartandstroke.com/site/c.ikIQLcMWJtE/b.3532069/k.5F46/Anatomy\\_of\\_the\\_Heart.htm](http://www.heartandstroke.com/site/c.ikIQLcMWJtE/b.3532069/k.5F46/Anatomy_of_the_Heart.htm)

In designing an active filter, it is difficult and cumbersome to include an inductor in an integrated circuit. However, the desired filter characteristics can be achieved by replacing the inductor with a high-performance operational amplifier, also known as op-amp. In building the active band pass filter, an op amp is used in its inverting configuration. A fast roll-off in the low frequency range is needed for this filter to ensure the DC offset is removed while saving the normal heart rate signal. The exact circuit block for this stage is shown in Figure 8 below.

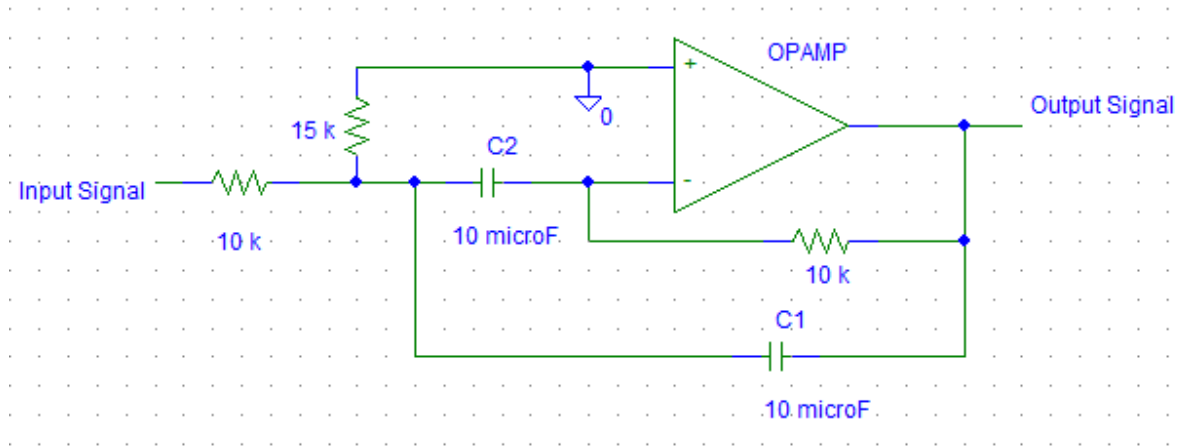


**Figure 8 - Active Band Pass Filter Circuit**

In the above circuit the 15 kΩ resistor is added to allow an additional degree of freedom in being able to easily modify the gain and the center frequency. The gain of the active band pass filter with matching capacitors can be described by the equation below.

$$A(s) = -\left(\frac{2Q}{1 + \frac{10k\Omega}{15k\Omega}}\right)\left(\frac{sw_o}{s^2 + s\frac{w_o}{Q} + w_o^2}\right)$$

$$A(w_o) = -\frac{1}{2}\left(\frac{10k\Omega}{15k\Omega}\right)$$

**Equation 4 – Filter response equations with center frequency equal to  $w_o$  [11].**

Plot of the magnitude of the transfer function is presented in figure 9 below. A gain of -0.5 is chosen for this circuit to avoid over amplification of the signal. The reason for this is that the filtered signal is sent to a summing amplifier to add an offset such that the output of the summing amplifier is a positive signal. An offset added to a large signal would shift the signal higher than

what can be realized due to the source voltage. Therefore, any necessary amplification of the signal is achieved at the last stage of the hardware circuit.

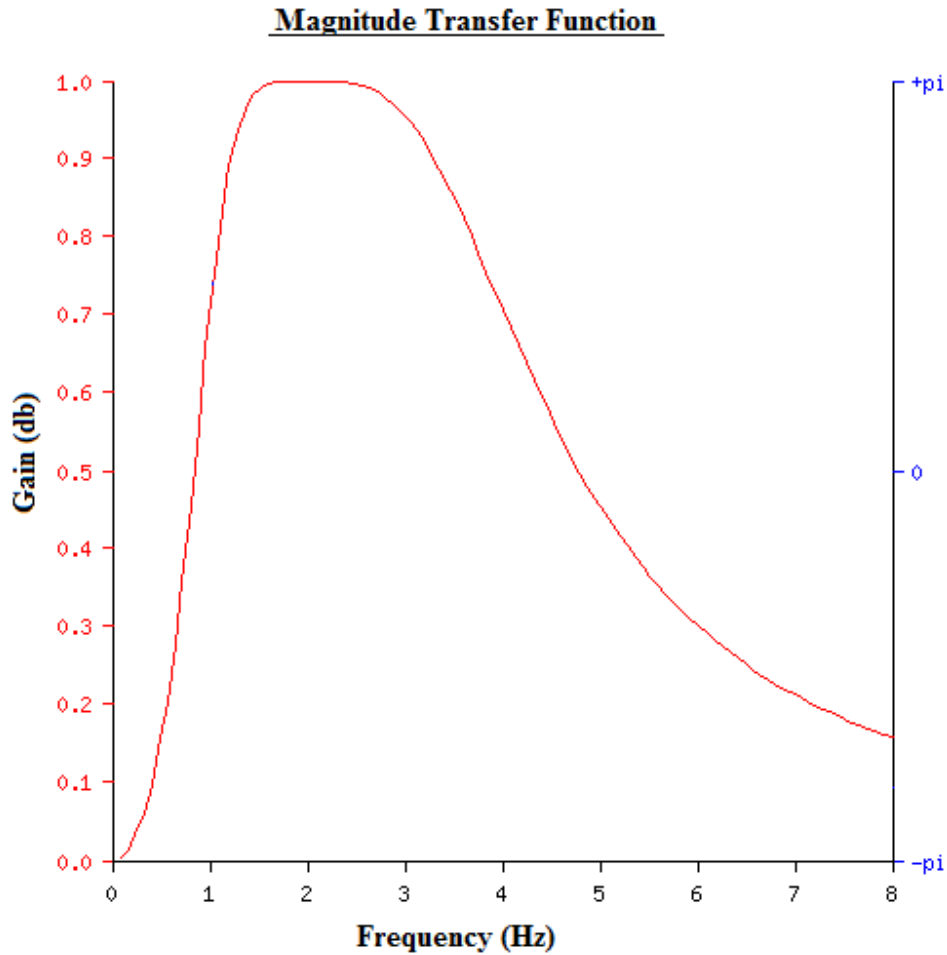


**Figure 9 - Magnitude transfer function for the active band pass filter**

#### *4.7 Passive Signal Filtering*

Although, the high performance and a sharp roll-off of the active band pass filter is desired for a clean PPG waveform to measure the peak height and pulse transit time, this filter results in the attenuation of the breathing rate signal. The low frequency respiratory induced intensity variations in the photo diode optical signal provide the mechanism for measuring the breathing rate. Therefore, the active band pass filter in the previous stage needs to be replaced by a passive filter to detect the PPG modulation waveform.

A passive band pass filter is easy to design and implement. Frequency response of a single pole low pass filter is given by equation 5 below.

$$f_{CLP} = \frac{1}{2\pi RC}$$

**Equation 5 – Cut-off frequency of a single pole low pass filter**

Using the above equation specific values for the resistors and capacitors are calculated. The complete circuit block for the passive band pass filter used at this stage is illustrated in Figure 10.

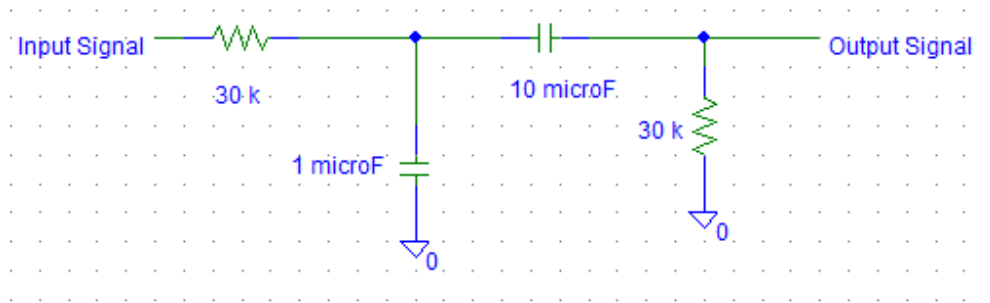


**Figure 10 - Passive band pass filter**

The bandwidth of above passive band pass filter is 0.53 Hz to 5.3 Hz.

#### *4.8 Summing Amplifier*

The voltage signal at this stage is in the milli-Volts range. The signal is filtered to remove the external ambient noise as well internal artifacts. However, this signal is not ready to be sent to the microprocessor to be converted to the digital form. The analog to digital converter requires that its input signal be entirely positive. The signal received from the band pass filter at this stage is between -1 mV to 2.25 mV. A DC offset needs to be added to this signal to ensure it remains positive.

A positive voltage signal needs to be added to the incoming PPG signal. This can be accomplished using a summing amplifier. Two input voltage sources can be connected to the inverting terminal of the amplifier. Since no current enters the operational amplifier at the negative or the positive terminal, currents due to the two input voltage sources are forced to be added and passed through the feedback resistor.

The second voltage source can be generated using the main input source voltage and a voltage divider. The complete circuit block is presented in Figure 11.

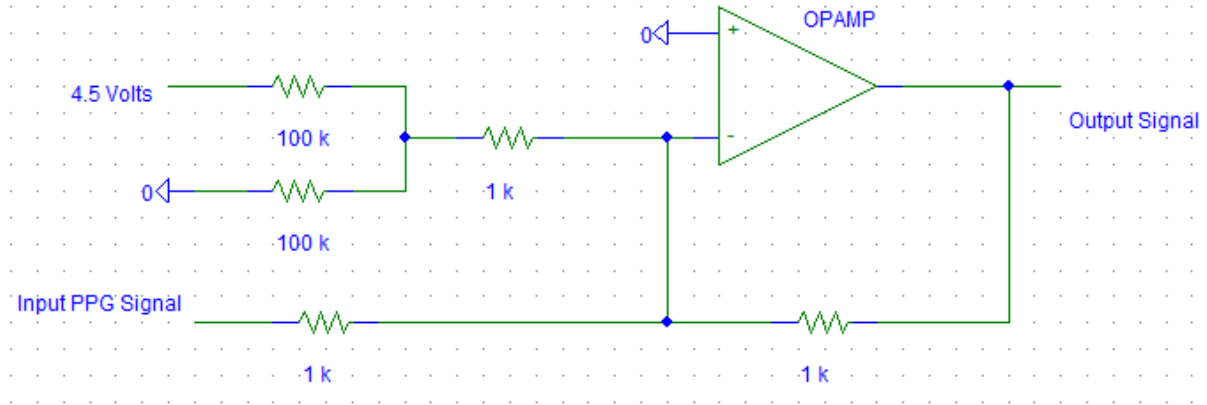


**Figure 11 - Summing Amplifier**

$$V_{out} = \frac{R_2}{R_1 + R_2} * V_{in}$$

**Equation 6 – Voltage divider**

Using equation 6, voltage being added to the input PPG signal is calculated to be 2.25 volts. An addition of a bigger offset caused the signal to be cut off at the peaks, thus the minimum needed DC offset was added to ensure successful transmission to the microprocessor.

#### *4.9 Final Amplification*

Although, the signal at this stage is positive, it is still in the milli-Volts range. For efficient analog to digital conversion of the signal, it must be amplified before sent to the microprocessor.

##### 4.9.1 Measuring the Pulse Height and Pulse Transit Time

The phase shift of 180 degrees caused the initial amplifier gets reverted by the active band pass filter. Thus, the gain at this stage should be achieved by the use of a non-inverting amplifier. The non-inverting amplifier is constructed using the operational amplifier by feeding in the input voltage signal to the positive terminal of the op-amp. A part of the output voltage of the op-amp is used as feedback into the negative terminal. Again, to realize this non-inverting amplifier, it is



assumed that the operational amplifier is ideal and the current fed into the negative terminal of the op-amp is zero. The resulting gain is given by the equation 7.

$$A_v = 1 + \frac{1\text{ M}\Omega}{1\text{ K}\Omega}$$

**Equation 7 – Gain of an non-inverting amplifier**

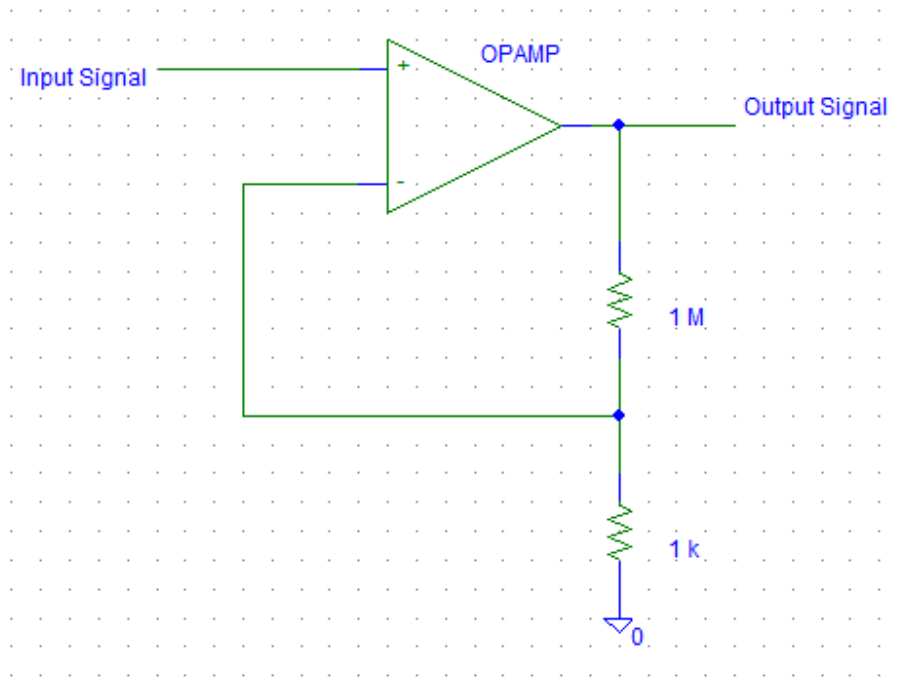


**Figure 12 - Non-inverting amplifier circuit**

The circuit to achieve a 1000 times gain is accomplished using the circuit shown above in figure 12. This gain is necessary to ensure that the signal passed to the microprocessor is in the Volts range. It can be noted from equation 7 that the addition of 1 Volts ensures that the gain is positive. Since, the resistor values are pure real no phase shift results in the output signal of this amplifier.

#### 4.9.2 Measuring the Breathing Rate

To calculate the breathing rate, the low frequency respiratory induced intensity variations in the photo diode need to be preserved. For this reason, the active band pass filter was replaced by the passive band pass filter. Therefore, the initial phase shift of 180 degrees caused by the

preamplifier does not get corrected. To correct for this phase shift the final amplification block designed in the previous section is replaced by an inverting amplifier. Since the gain of the inverting amplifier is negative, the 180 degree phase flip produces the desired corrected signal at the output. The circuit for this final amplifier is presented in figure 13 below.

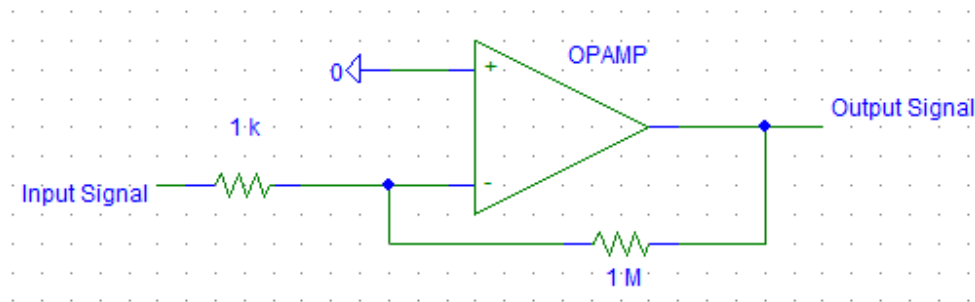


**Figure 13 - Final amplification block for the breathing rate calculation**

#### 4.10 Breathing Rate Envelope Detection using Hardware

The variations caused by the breathing rate modulate the amplitude of the PPG waveform. To measure the breathing rate, the envelope of the modulated PPG waveform needs to be extracted. The envelop detection can be done using a simple diode in series with a block of a capacitor parallel to a large resistor. The circuit for this configuration is shown in Figure 14. The condition to recover the envelope is that the modulated signal must have frequency components much higher than the modulating signal; this is true with breathing rate. A normal breathing rate is around 30 breaths per minute which corresponds to 0.5 Hz. The lower range of a normal heart rate for an athlete is around 40 beats per minute corresponding to 0.67 Hz. For proper envelop detection, the time constant for the circuit in Figure 14 needs to be faster than the breathing rate but slower than the heart rate.

**Table 2 - Time Constant Determination Chart**

Breathing Rate (Breaths/minute)	Time Constant ( $R_f \cdot C$ )	Heart Rate (Beats/minute)
12 bpm – 30 bpm 0.2 Hz – 0.5 Hz	2.5 seconds 0.4 Hz	40 bpm – 210 bpm 0.67 Hz – 3.5 Hz

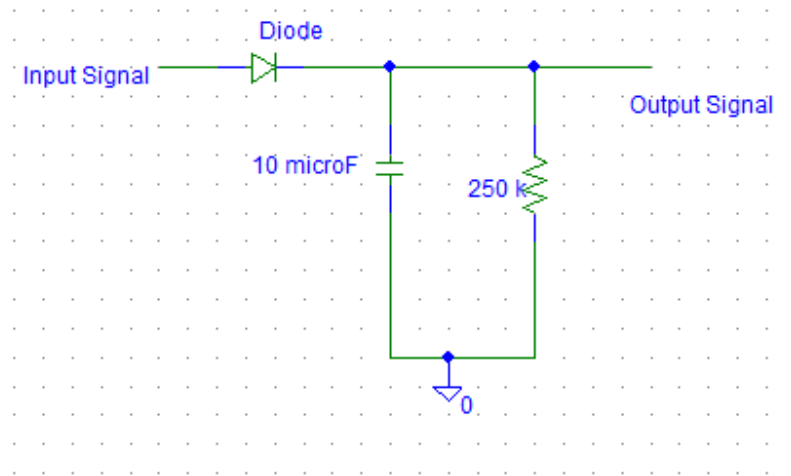


**Figure 14 - Envelope Detection Circuit**

The resistor and capacitor values for the circuit in figure 14 are determined using the frequency limitation defined in table 2. The forward voltage of the diode is 0.7 Volts. On the positive half cycle of the modulated PPG waveform the diode turns on and the capacitor charges quickly. On the negative half cycle, the diode turns off and the capacitor discharges slowly through the 250 k $\Omega$  resistor. As this process happens periodically the capacitor voltage follows the envelope of the received signal. To ensure that the envelope is detected, the capacitor is chosen such that its charging time is small compared to the 1/minimum-heart-rate. The capacitor must also discharge slightly between the periods but faster than 1/highest-breathing-rate.

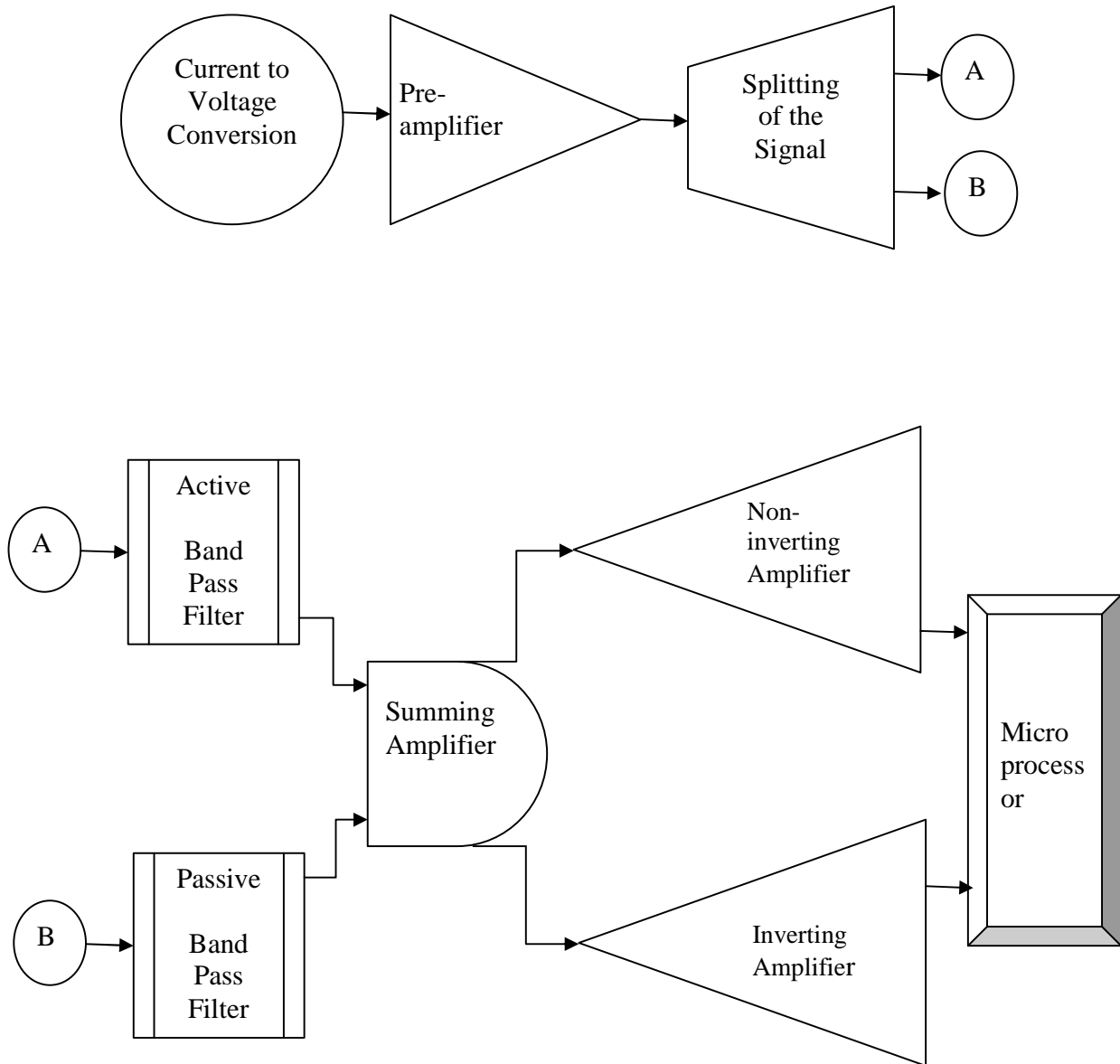
Although the circuit block for envelop detection is easily designed, its implementation is very difficult. This is because it requires the preservation of frequency components above 0.2 Hz. However, as noted in the previous sections the received PPG waveform experiences noise interference from multiple sources which need to be removed using a band pass filter. Since the preservation of the breathing rate variations necessitated the use of a passive filter, the noise in the output signal is too prominent for the above described circuit in figure 14 to provide as useful envelope detection as can be extracted using software techniques. Therefore, the output of the inverting amplifier is used to extract the envelope from the PPG waveform in MATLAB.

#### *4.11 Breathing Rate Envelope Detection using Software*

The fast Fourier transform (FFT) in MATLAB provides the frequency domain representation of

the time domain signal. This operation applied to the modulated PPG waveform presents all frequency components in the signal. Zeroing all frequency above the maximum breathing rate frequency provides the modulating envelope.

#### 4.12 Complete Hardware Circuit



## 5 RESULTS AND DISCUSSION

This section focuses on testing procedures and the results obtained. Since the implemented hardware circuit is non-invasive and does not pass any sort of electrical signal to the user, the device is safe to use.

### *5.1 Testing*

The testing subject was a healthy 23 year old male university student, Omer Waseem. Omer is a member of the NIHMS team who designed and implemented the microprocessor and the Bluetooth hardware as well as the software components.

Although much of the noise was filtered using the band pass filter some noise was still present in the signal. The sources of this noise were ambient light and motion artifact. Omer was asked to remain as calm and still as possible. The impact of the ambient noise was reduced by covering Omer's finger with a dark cloth after the photo diode and the emitter were attached. While this significantly cleaned the PPG waveform on the oscilloscope further stability was required. Holding the photo diode and emitter in the other hand introduced motion artifact due to unavoidable tremor. To minimize this artifact a proper transducer was required to keep the photo diode and emitter in place.

To obtain a good waveform, the photo diode and the emitter had to be placed very close to each other with a specific orientation. This further increased the need for a transducer. The first prototype of the transducer was built using Styrofoam. It was used because of the flexibility it provides in positioning the diodes. The Styrofoam also helped in covering the photo diode from ambient light. The leads of the photo diode and emitter were separated using electrical tape to avoid having them touch each other. Though, the transducer worked well for detecting the PPG waveform on the tip of the index finger, the transducer did not work for the brachial site.

Two PPG waveforms are needed at two different sites along the arm length to determine the pulse transit time. Exact replication of the same hardware circuit with another transducer was needed to detect the waveform along the brachial artery. Since, Yousuf Jawahar, another member of the NIHMS team implemented the PPG hardware for the calculation of blood oxygen

saturation, his device was used to pick up the PPG waveform at the second site simultaneously. Though, the both of the circuits were able to detect the PPG waveform at the tips of the finger, none worked for the site along the brachial artery on the upper arm.

After an exhaustive number of testing trials a new design of the transducer was built using a small cup with a diameter size of 0.5 inches and a width of approximately 0.75 inches. Holes were made on the bottom of the cup to insert the leads of the diodes. The other topless end of the cup was attached to the brachial site on the arm. This transducer was less bulky than the Styrofoam, however, it was not easy to relocate the transducer to a slightly different position along the brachial artery. This transducer was also not helpful in detecting a PPG waveform anywhere along the upper arm.

A third transducer was built using a small flashlight. The flashlight was disassembled to remove the original components in it. The leads of the photo diode and the emitter were soldered to long wires and pushed through to the back of the flashlight. An illustration of this transducer is presented in an image in Appendix A. The front end of the transducer had a disk in it with circular holes. A diagram of this disk is shown in figure 15 below.

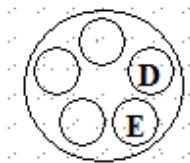


**Figure 15 - Front end of the flashlight transducer**

The photo diode is inserted in one of the holes and an emitter in the slot beside it. Note that all of the remaining holes are left empty. The length of the flashlight is about three inches while the wires soldered to the leads of the diodes are at least nine inches long. The extra lengths of the wires provide the necessary flexibility in easily repositioning the transducer to different sites along the brachial artery.

Although, a PPG waveform was not detected after the initial several trials of using the flashlight transducer along the brachial artery, the transducer was flexible enough to continue the testing at

other sites. An exhaustive set of trials eventually provided a small PPG waveform measured along the brachial artery near the left arm elbow.

The difficulty encountered in detecting the PPG waveform at a site on the upper arm was due to the excessive amount of tissue, bone and muscle mass present. The brachial artery is embedded in this mesh and so it does not receive the light emitted by the LED in a sufficient quantity. For the same reason, a huge fraction of the light gets lost in transmittance through tissue or is returned as reflectance resulting in a large DC output signal. Once a site along the arm near the elbow was found it was marked with a pen. A picture of this marked site is included in Appendix A.

The device and the transducer were tested with several individual and consistent results were received. A PPG waveform was easily detected along the tip of the finger but a few trials were needed to pick up the PPG signal from the brachial site.

Furthermore, the hardware circuit designed for the breathing rate envelope detection was tested however, unsatisfactory results are obtained. The amount of noise filtering needed to be reduced to allow the respiratory induced variations in the PPG waveform to be noticeable. This largely decreased the signal to noise ratio. Amplification of the signal did not aid as it would also amplify the noise embedded in the signal. After fine tuning the cut off frequencies of the filters a noticeable modulation of the PPG waveform by the breathing rate was observed. Hardware approach to envelop detection was replaced by MATLAB software as it provided a much cleaner envelope.

## *5.2 Hardware Results*

This section includes results obtained from the hardware before any data processing is performed. In order for the analog to digital converter to properly sample and convert the signal, much of the noise had to be filtered in the hardware stages. Figure 16 below shows the finger PPG waveform observed on the oscilloscope. The signal appears to very clean because the dicrotic notch is clearly visible. The signal has amplitude of 1.28 Volts.



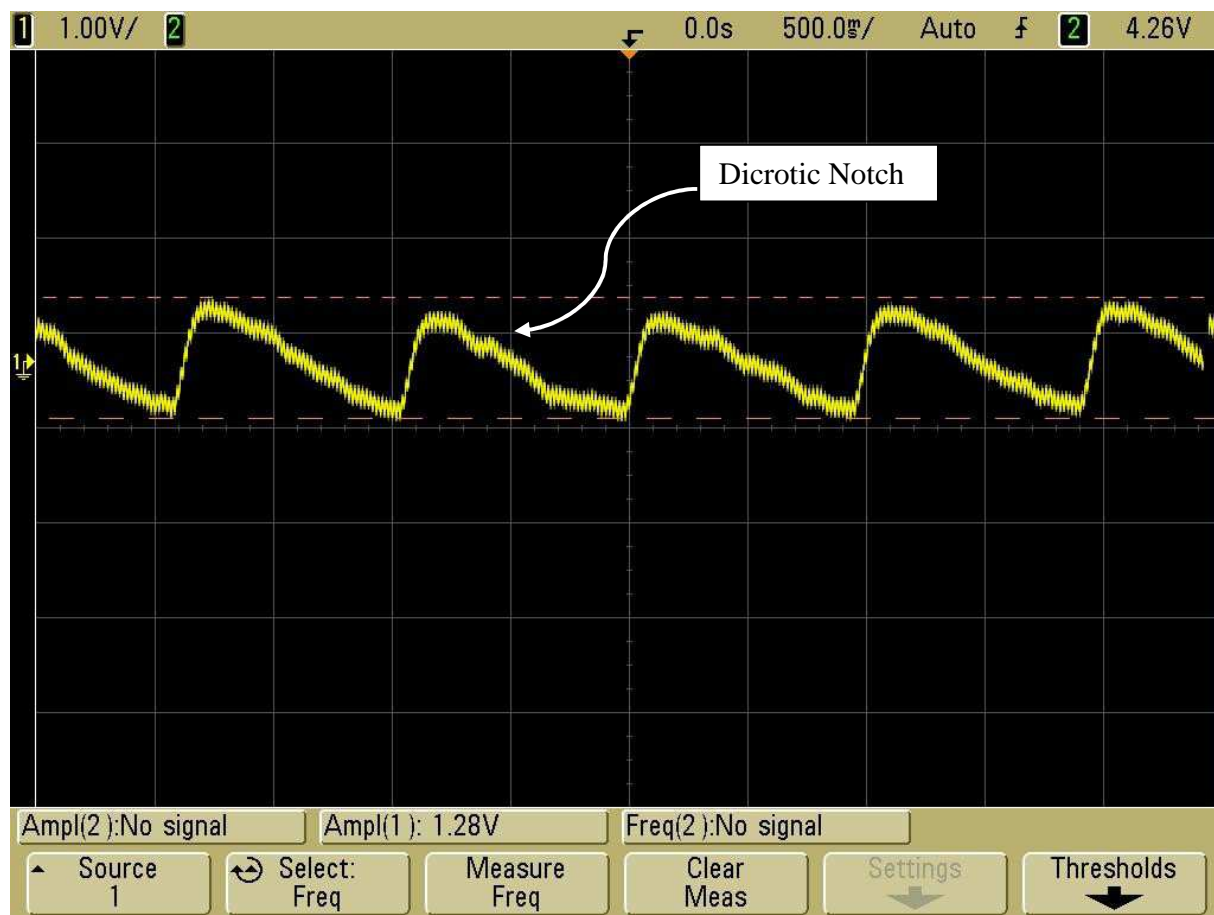


**Figure 16 - Finger PPG waveform observed on the oscilloscope**

The above figure is the test result of Yousuf Jawahar's finger PPG waveform. This waveform can be used to calculate the heart rate variability and to measure the peak height. However, a single PPG waveform is not useful enough as it does not provide the pulse transit time.

Two PPG waveforms were taken at two sites on Omer Waseem's left arm simultaneously. The exact location on the upper arm is identified in an image included in Appendix A. The resulting waveforms observed on the oscilloscope are presented in figure 17 below.

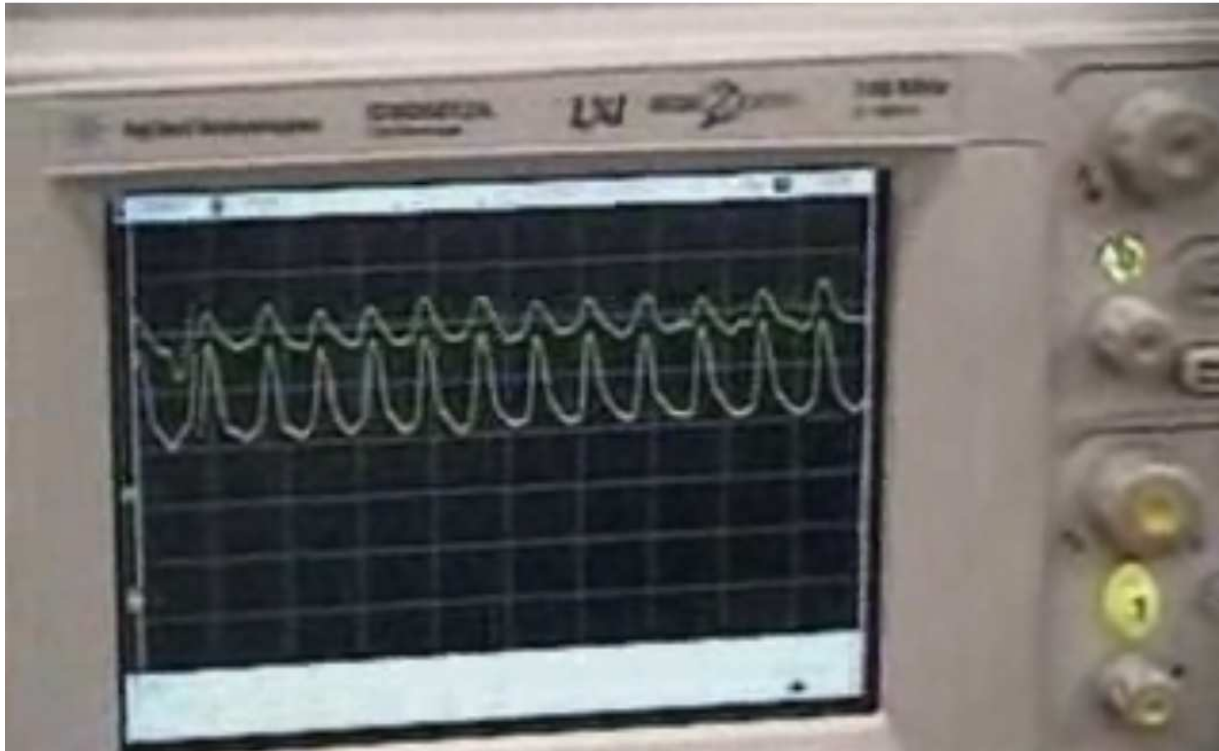


**Figure 17 - Brachial PPG (top), Finger PPG (bottom)**

Real time clean PPG signals in Figure 17 from hardware filtering alone proves the successful working state of the developed hardware. The top waveform is the brachial PPG and the bottom is the finger PPG. The traditional sphygmomanometer's cuff was placed on Omer's right upper arm to determine his systolic and diastolic blood pressure at the same time as receiving the two PPG waveforms. The purpose of this trial was to determine the correlation coefficient between the actual SBP/DBP and the PPG peak height and pulse transit time. His heart rate recorded at the time along with several blood pressure readings are tabulated below in table 3.

**Table 3 - Physiological Data obtained from the Sphygmomanometer**

Trial	Systolic Blood Pressure (mmHG)	Diastolic Blood Pressure (mmHG)	Heart Rate (Beats Per Minute)
1	126	73	68
2	129	71	73
3	131	83	68
4	137	70	72
5	121	70	65
6	111	67	63
Average:	126	72	68

### *5.3 Signal Transmission from Hardware to Computer*

After the final amplification stage the PPG waveform signal is sent to the microprocessor. The analog signal is converted to the digital form and is sent to a computer using Bluetooth transmission. The incoming real time signal that gets sent to the computer is sampled at the rate of 27 milliseconds. The factor that influences the sampling rate the most is the serial transmission between the PIC and the Bluetooth module.

### *5.4 Digital Filtering*

Although, the hardware removes much of the noise, the signal sent to the computer requires further cleaning before the peak height or pulse transit time can be calculated. Figure 18 below shows 200 samples of the two PPG waveforms measured for Omer Waseem in the above mentioned trial.

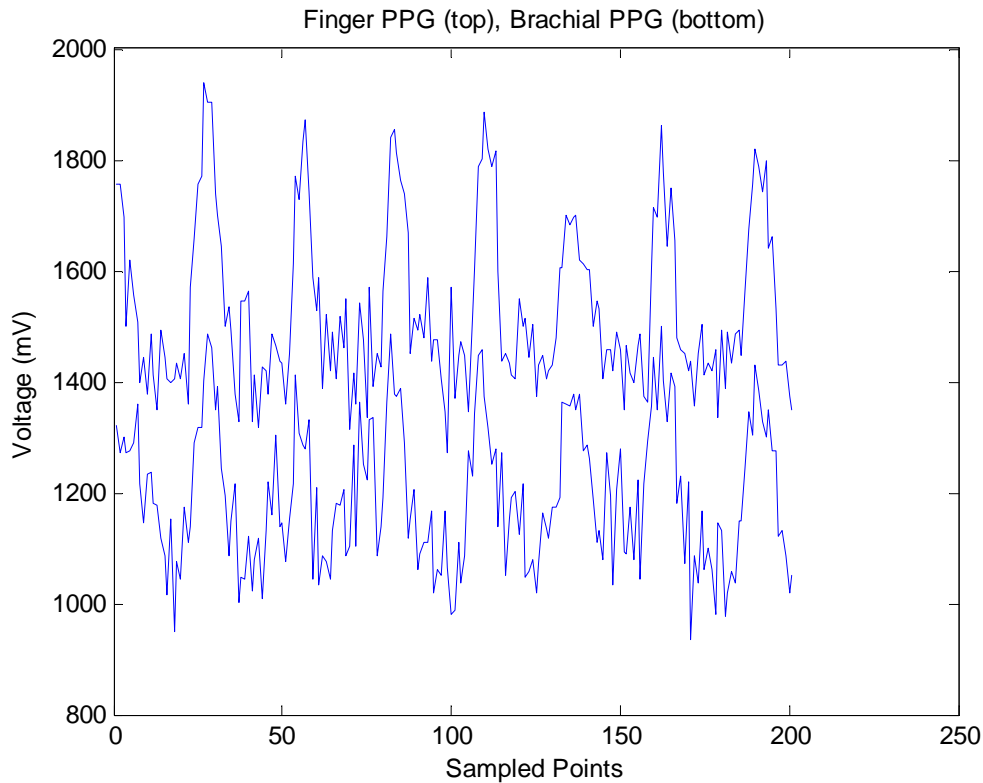


**Figure 18 - Raw PPG signals as sent to the computer**

Since it is much easier to filter the data in the frequency domain, the raw obtained data is transformed to the frequency domain using MATLAB's fast Fourier transform (FFT) operation. In the interest of measuring the PPG peak height and pulse transit time, the signal is filtered to remove any frequency components higher than 3 Hz. It is worth noting that from the data collected in 6 trials the highest heart rate was below 90 beats per minute corresponding to 1.5 Hz. Digital filtering significantly cleans the above shown signals. Four hundred points of digitally filtered two PPG waveforms are presented in Figure 19.

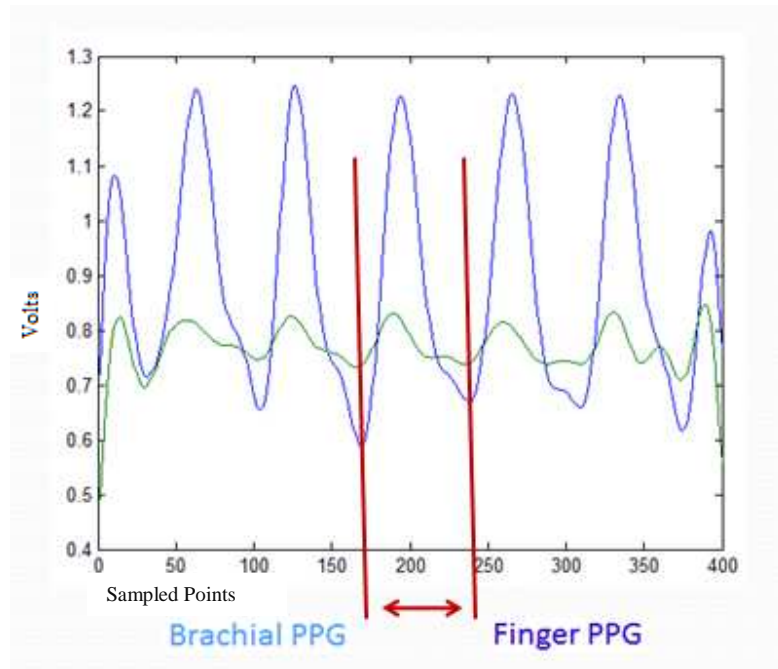


**Figure 19 - Digital filtered finger PPG (blue) along with the brachial PPG (green)**

### *5.5 Peak Detection Algorithm*

The above signals are filtered enough such that the peak heights and pulse transit time can be calculated. However, before these calculations can be performed, peak detection algorithm is needed. The algorithm is presented in the flow chart below. The chart compares three points and a set of three points resulting in a peak are shown in Figure 20.

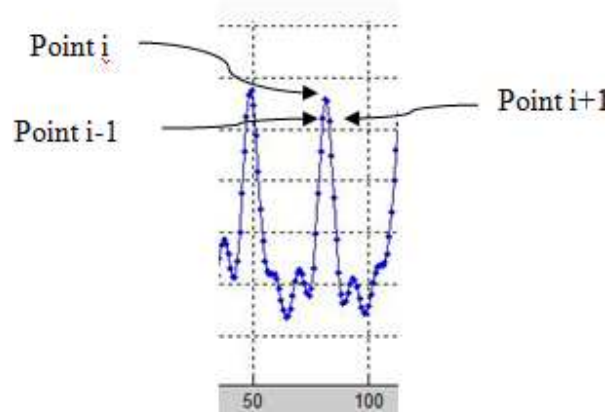
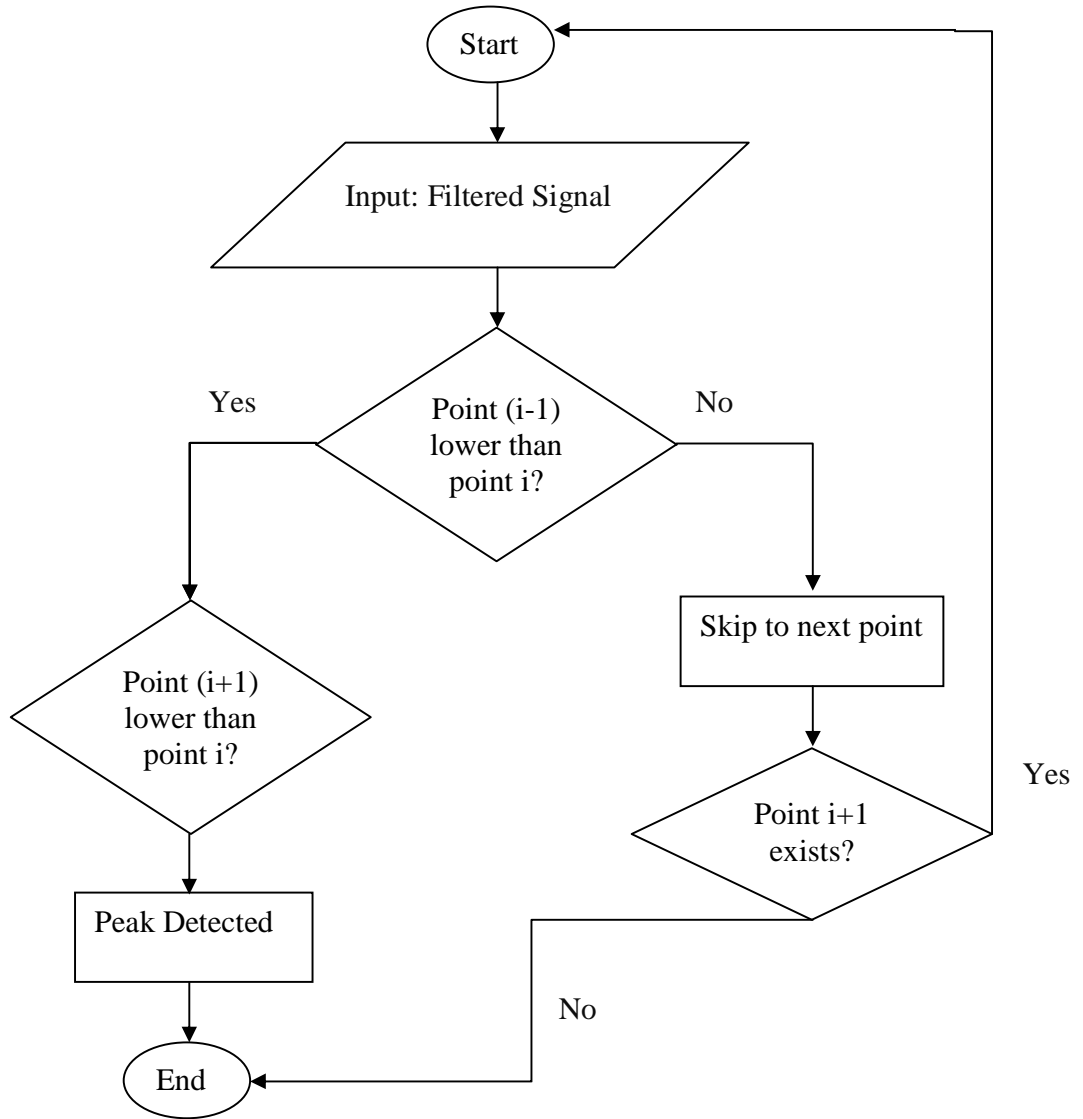


**Figure 20 - Three points compared in the peak detection algorithm**



**Flowchart 1 – Peak Detection Algorithm**

Once the peak is detected the then corresponding time instant is used to calculate the instantaneous heart rate. Equation 8 below shows the exact calculation performed.

$$IHR = \frac{1 \text{ beat}}{\text{Peak } i + 1 \text{ arrival time} - \text{Peak } i \text{ arrival time}} * \frac{60 \text{ seconds}}{1 \text{ minute}}$$

**Equation 8 – Calculation of the instantaneous heart rate**

### 5.6 Arterial Blood Pressure Calculation Using Pulse Height

Once a peak is detected then the peak height is simply the amplitude at the maximum point minus the amplitude at the end of the diastolic time. The peak height in Figure 21 is 199 mV.

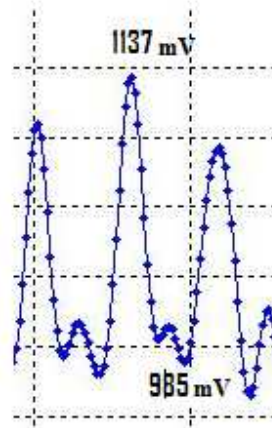


**Figure 21- Peak amplitudes to determine peak height**

Correlation coefficients between the systolic and diastolic pressure readings can be calculated using the actual values obtained using the sphygmomanometer.

**Table 4 - Test Values obtained for Calibration**

Health Factor	Omer Waseem's Actual Values
Systolic Blood Pressure	131
Diastolic Blood Pressure	83
Heart Rate	68 beats per minute

**Table 5 - Calibration Factors for to determine SBP and DBP**

Calibration Factor	Omer Waseem
SBP Correlation Factor	$1137/131 = 8.67$
DBP Correlation Factor	$935/83 = 11.26$
SBP, DBP difference Correlation Factor	$(1137-935)/(131-83) = 4.21$

Calculations of instantaneous blood pressure values calculated using the correlation coefficients determined for the peak height for peaks 6 and 11 in Figure 22, are presented in table 6.

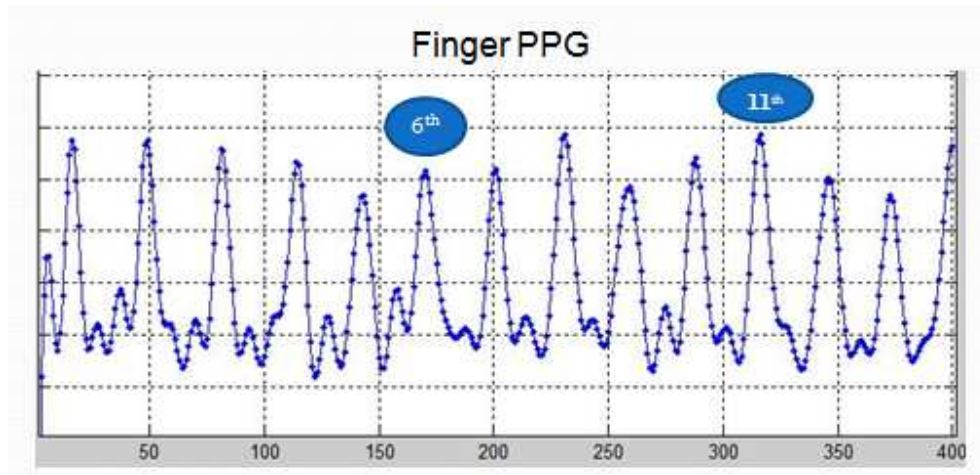


**Figure 22 - SBP and DBP values calculated for the labeled peaks**

**Table 6 - Blood Pressure Calculations using the Pulse Height Correlation Coefficients**

<b>6<sup>th</sup> Peak</b>	<b>11<sup>th</sup> Peak</b>
SBP: $1108/8.67 = 128$	SBP: $1143/8.67 = 132$
DBP: $938/11.26 = 83$	DBP: $917/11.26 = 81$
$178/4.21 = 40$	$226/4.21 = 54$
$128-83 = 45$	$132-81 = 51$

### *5.7 Arterial Blood Pressure Calculation Using Pulse Transit Time*

Pulse transit time is measured as the interval between the trough of the brachial PPG to the respective trough of the finger PPG. This interval is identified in figure 19 on page 35. Table 7 below shows the correlation coefficients between the SBP/DBP values and the PTT. Table 8 presents sample calculations for two peaks. Stability of the correlation coefficients is tested by graphing the calculated SBP values for consecutive peaks in Figures 23 and 24.



**Table 7 - Correlation Coefficients for Pulse Transit Time**

Calibration Factor	Omer Waseem's Data
SBP, DBP difference Correlation Factor (SDcorr)	$(1137-935)/(131-83) = 4.21$
DBP Correlation Factor	$83/35 = 2.37$
Systolic BP Measurement	$(1137-935)/SDcorr + DBP + 17$

**Table 8 - Instantaneous Blood Pressure Calculations for two peaks using PTT**

6 <sup>th</sup> Peak	8 <sup>th</sup> Peak
DBP: $30 \times 2.37 = 71$	DBP: $27 \times 2.37 = 64$
SBP: $(1108-938)/4.21 + DBP + 17 = 128$	SBP: $(1143-939)/4.21 + DBP + 17 = 129$

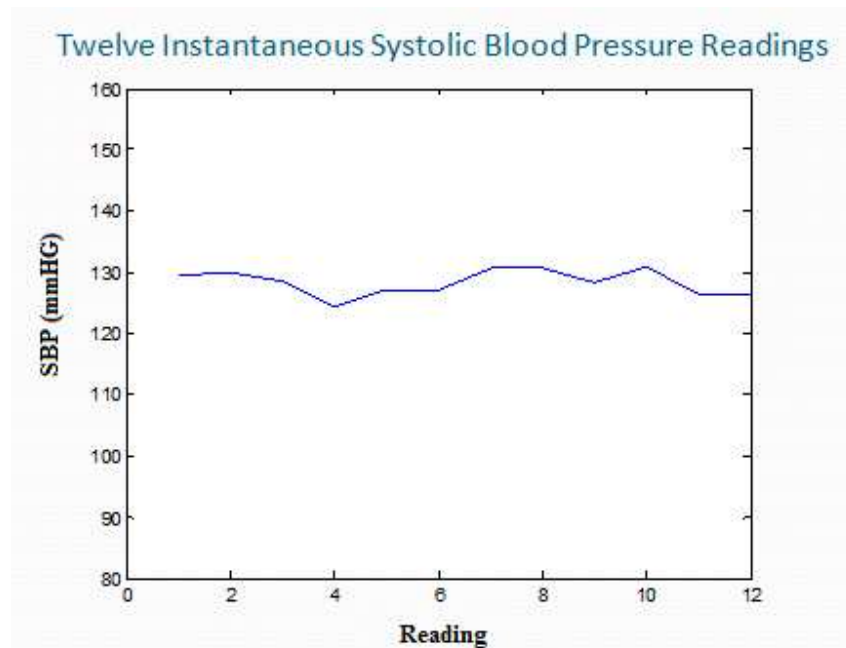


**Figure 23 - Stability of the correlation coefficients tested over the course of 12 peaks**

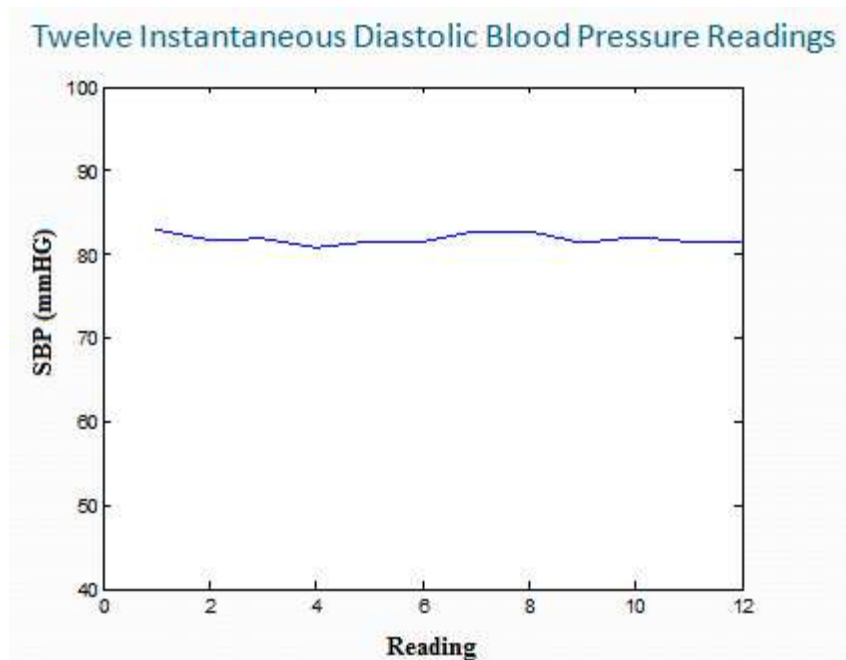


Figure 24 - Stability of PTT correlation coefficients observed through 12 consecutive SBP readings

#### 5.8. Heart Rate Variability Data Processing

HRV is calculated using standard deviation in MATLAB. Using a set of 12 consecutive IHR values the variations in HRV are shown in Figure 25.

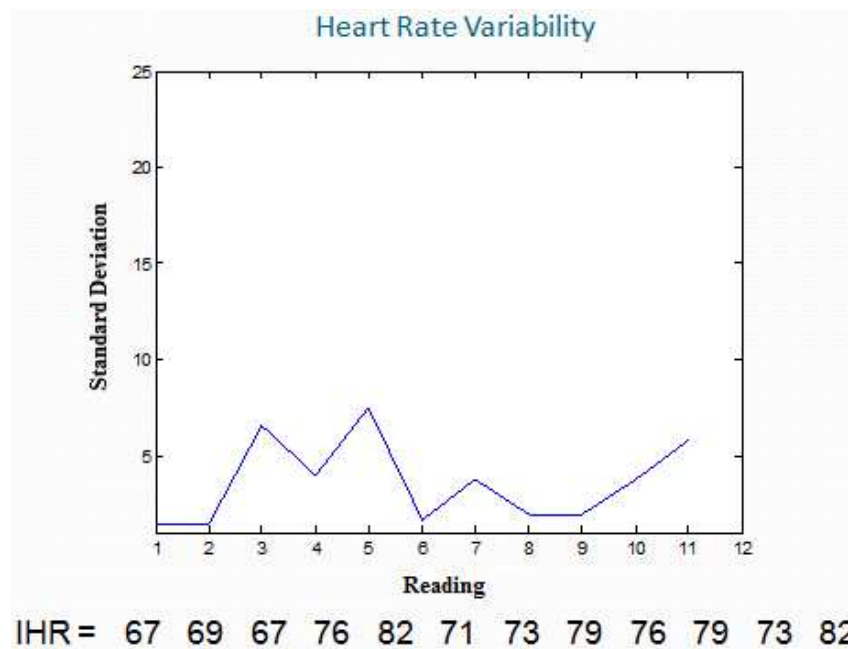


Figure 25 - HRV calculated using standard deviation and a set of IHR values

### 5.9 Instantaneous Breathing Rate Calculation

Attenuation of all frequency components above 0.35 Hz produces the envelope that modulates the PPG waveform. A set of 3000 values is presented in Figure 26 that show both the PPG waveform along with the breathing rate waveform.

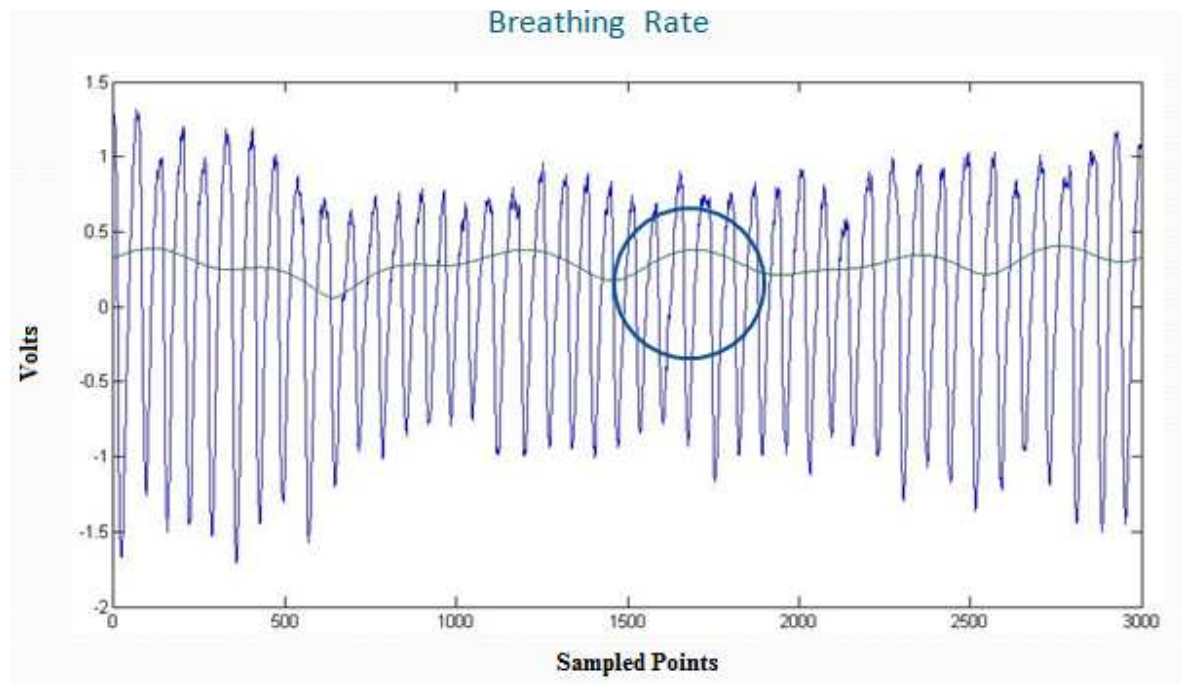


Figure 26 – Breathing Rate Measurement and envelope detection

$$\text{Breathing Rate} = \frac{1}{503 * 10ms} * 60 \frac{\text{seconds}}{\text{minute}} = 12 \text{ breaths per minute}$$

Equation 9 – Instantaneous Breathing Rate Calculation

The above equation 9 and figure 26 indicate that Omer's breathing rate at the trial time was 12 breaths per minute. This value is reasonable as Omer was in a resting state and this is confirmed with his heart rate of 68 beats per minute.

## 6 CONCLUSIONS

The problem stated in section 3 of designing and developing a non-invasive and safe device that allows instantaneous systolic and diastolic blood pressure values to be measured along with beat-to-beat breathing rate and heart rate variability was resolved within reasonable errors. There were hurdles such as difficult to filter interference due to ambient noise; however the biggest obstacle encountered was detecting the PPG waveform at the brachial site along the upper arm. Several transducers were built and many different test subjects were approached. An exhaustive set of trials eventually lead to a promising solution. Difficult to locate PPG waveform detection site along the brachial artery suggests that a robust transducer is absolutely necessary for the device to have usefulness in a clinical setting.

Since both the pulse height and pulse transit time could be measured once the PPG signals were digitally filtered, one was used to ensure the correctness of the calculated values using the other approach. Both of the approaches were necessary to find values for all unknown variables. The pulse height is the correlated difference between the systolic and diastolic blood pressure. However, knowing just the pulse height without the baseline blood pressure, specific values are difficult to compute. The pulse transit time varies inversely with the blood pressure. Thus, a baseline blood pressure using the pulse transit time can be used in the pulse height technique. Similarly, the difference in SBP and DBP from the pulse height can also be used to compute calculations in the pulse transit time approach.

Heart rate variability and breathing rate were both computed using the MATLAB software. Peak detection algorithm was used to identify the peaks of the PPG waveform. Identification of the peak provided a mechanism to extract detailed information about the peak which was used to calculate the HRV and BR.

The total project cost was \$45 Canadian dollars. A breadboard, diodes, capacitors, and resistors were purchased. The project was successfully completed in 7 months. A month was allocated to literary research, the hardware was built in 3 months, 2 months were spent on troubleshooting, and the last month was spent on data processing in MATLAB.

## 7 RECOMMENDATIONS

A robust transducer is absolutely crucial for PPG detection from the brachial artery. An in depth knowledge and creativity should be employed in designing the transducer. While all things may be considered on paper to produce the best seeming design, it may still fail in testing. Therefore, exhaustive testing trials must be performed to produce an improved design.

Biological signals are not only miniscule in quantity they are highly prone to noise and artifacts. Sometimes, the noise interferes with the signal of interest in such a way that any attempt to remove the noise will also attenuate the signal that needs to be measured. This was the case with detecting the modulating envelope in the PPG waveform to calculate the breathing rate. Thus, a software approach was used for envelope detection.

Additional literature research showed that the low frequency respiratory induced variations in the PPG waveform may also be caused by the autonomic nervous system involvement. During inhalation the stretch receptors in the lungs send a message to the pons in the brain through the vagus nerve to initiate exhalation and avoid over inflation of the lungs. The vagus nerve is part of the autonomic nervous system that influences the heartbeat. Inhalation inhibits the vagus nerve and so the heartbeat increases. The opposite effect is observed during exhalation. Modulation of the PPG waveform due to this factor is termed respiratory sinus arrhythmia (RSA) [12]. This knowledge can be used to measure additional physiological information about RSA and ANS.

Knowing the spectral or temporal properties of a noise signal provides information which can be used to design a filter. However, motion artifact is a type of interference for which the spectral information is not always known. The solution to this problem can be provided through the use of adaptive filters. The adaptive filter changes according to the change in noise. It can work as a notch or a comb filter. The noise however needs to be additive in order for most of the adaptive filters to work.

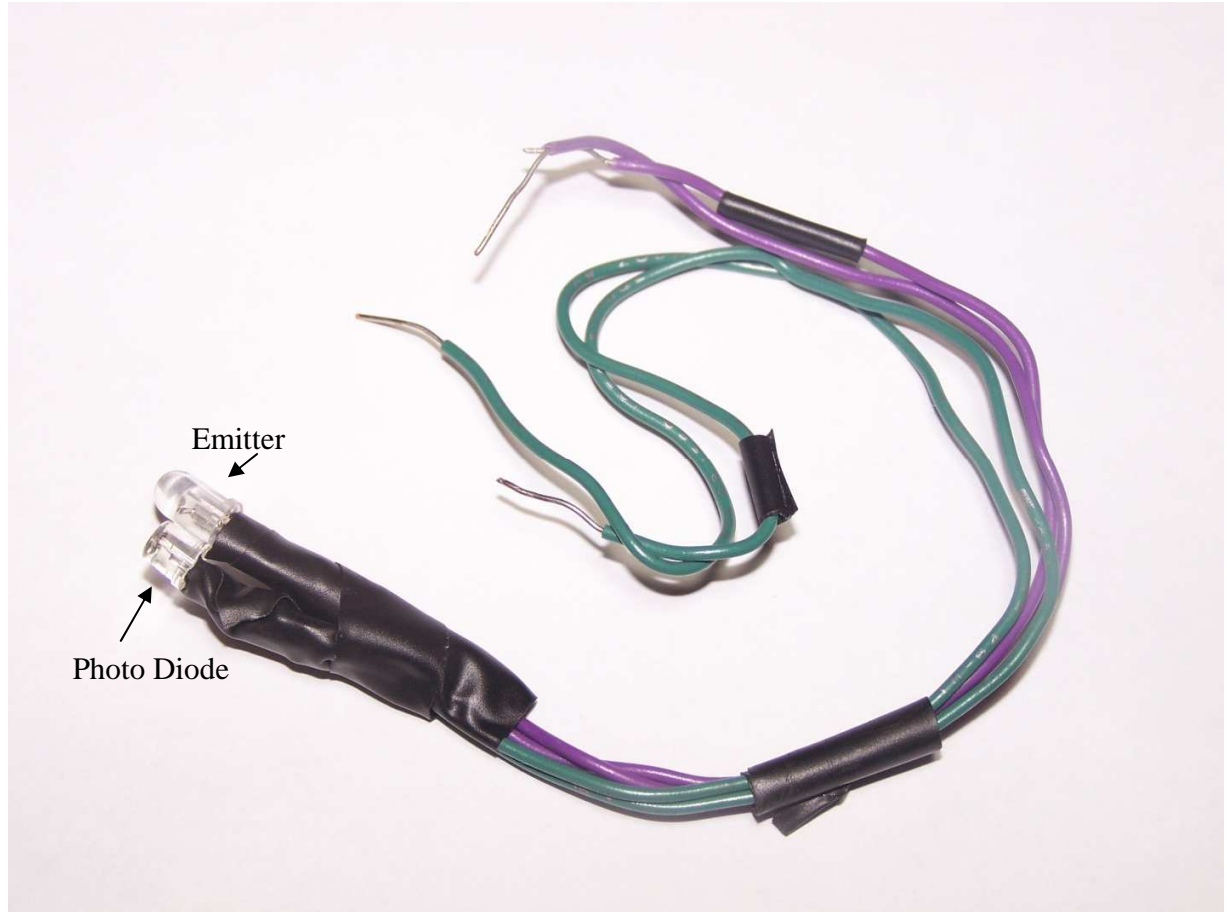
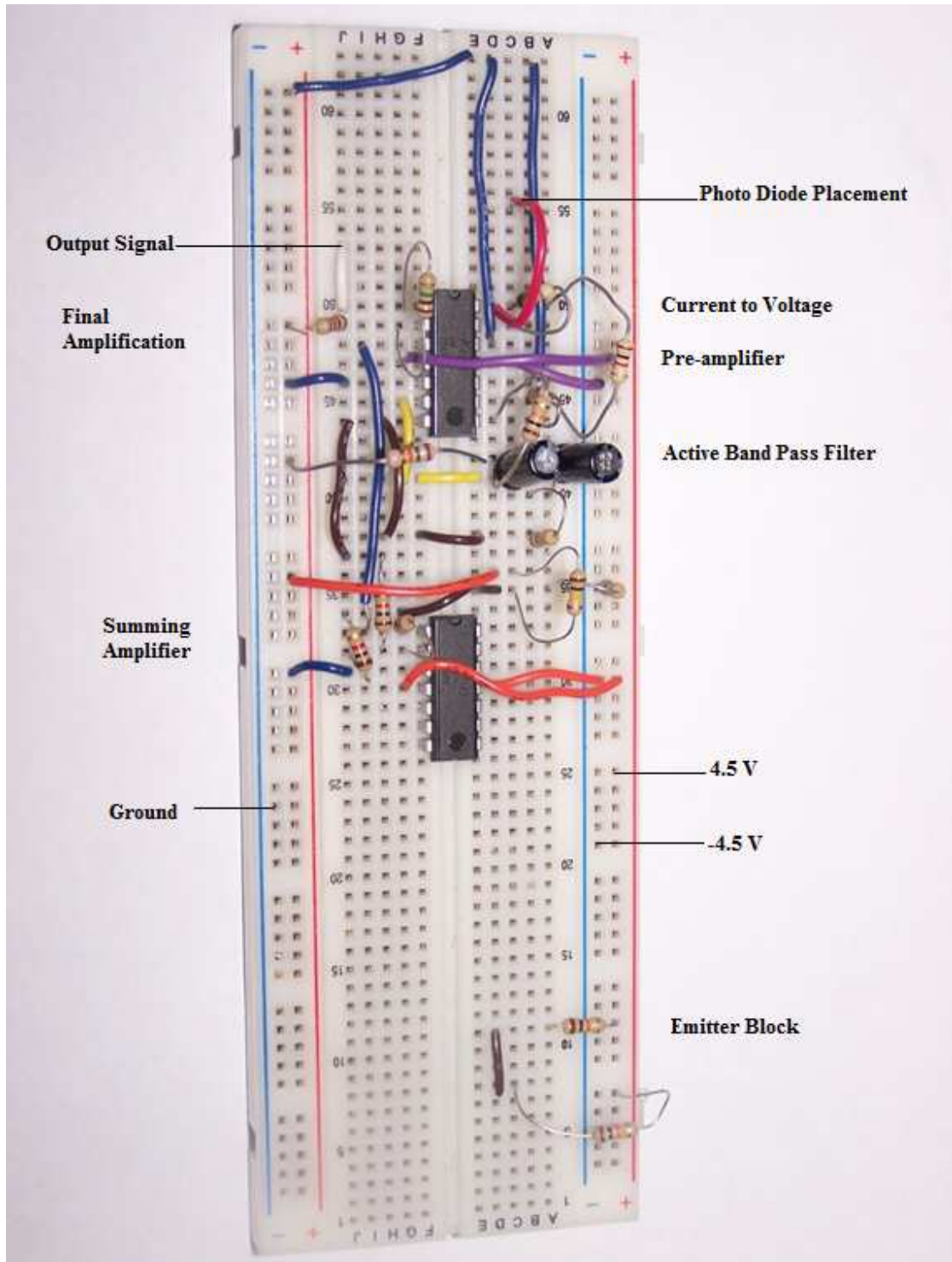
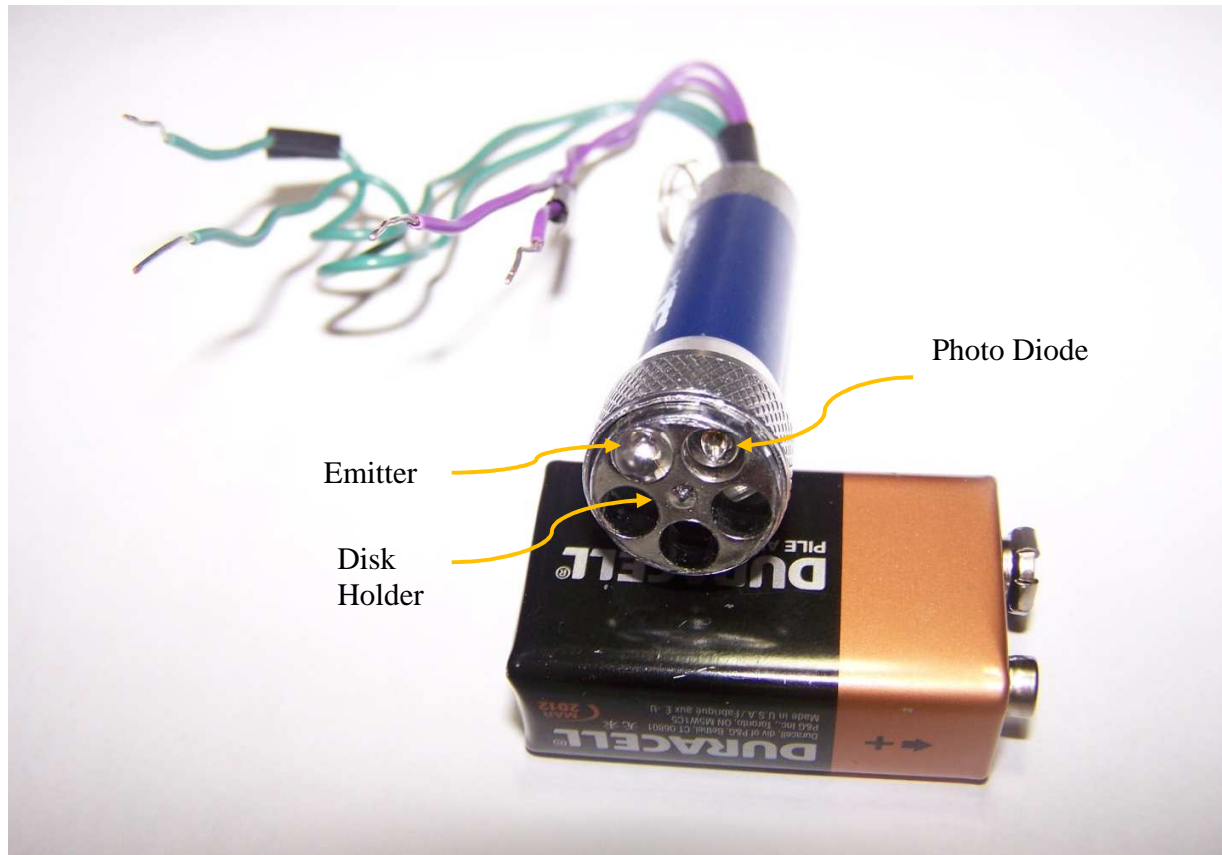


Figure 27 - First PPG Transducer



**Figure 28 - Device Hardware Complete Circuit Block**



**Figure 29 - An Improved Transducer**



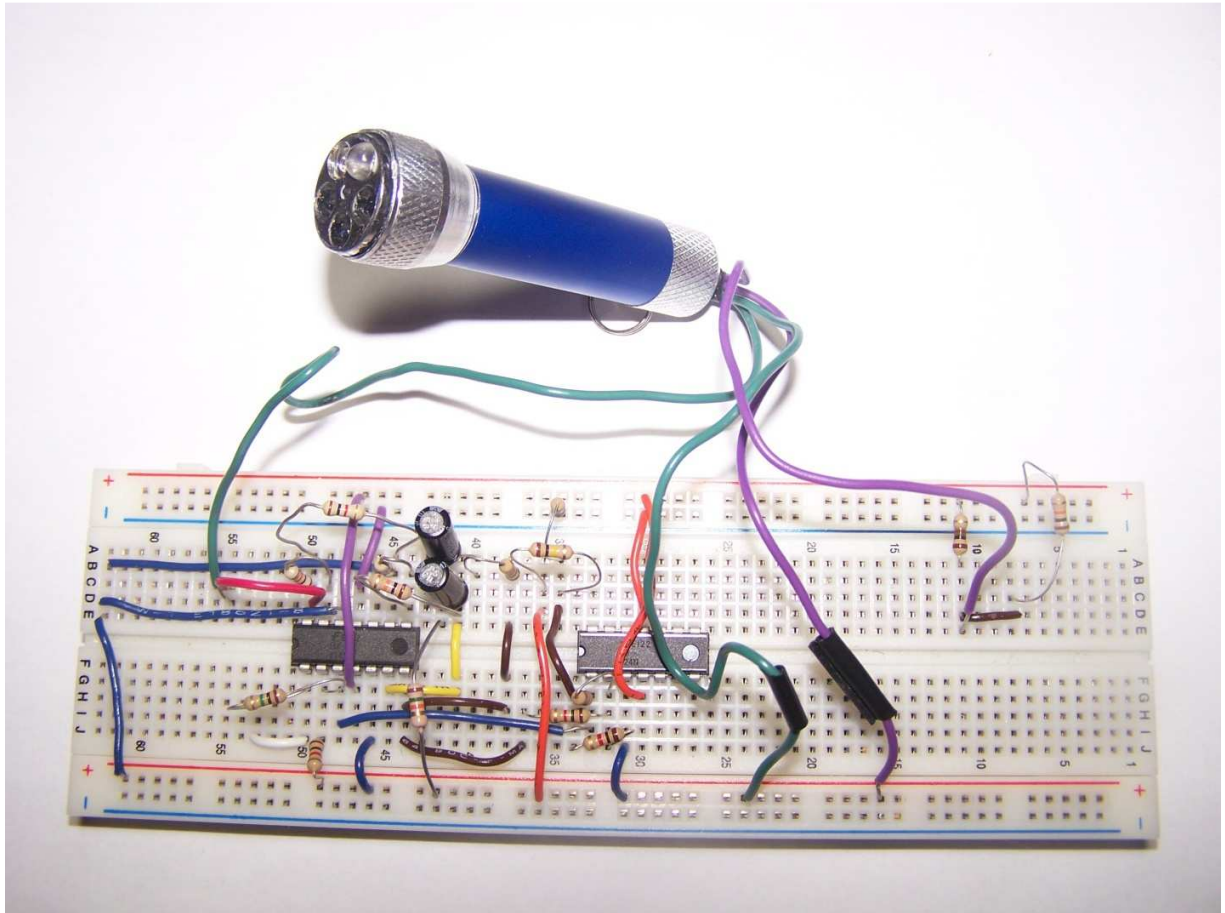


**Figure 30 - Device Hardware Prototype with the Transducer**

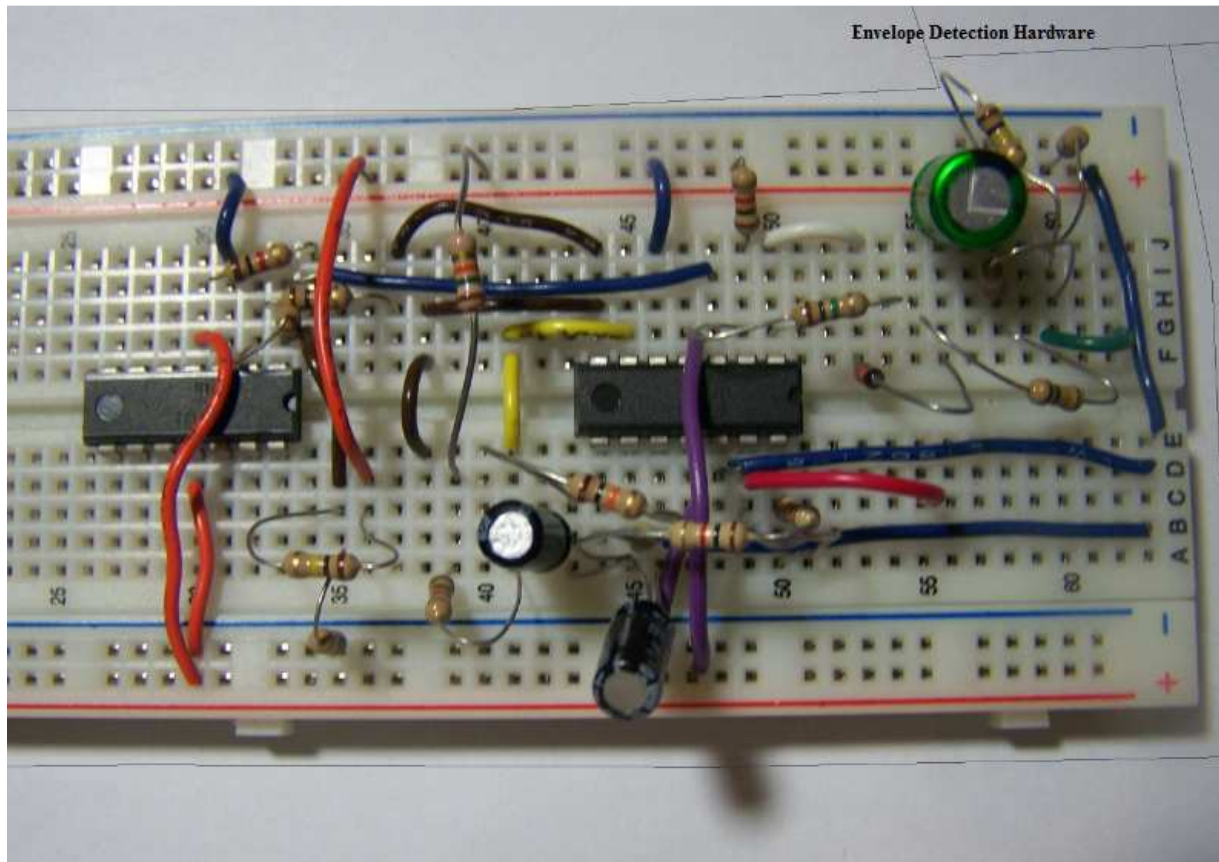


**Figure 31 - Hardware Prototype for Breathing Rate Envelope Detection**



**Figure 32 - Site for Brachial PPG Detection**

## 9 APPENDIX B: DATA PROCESSING IN MATLAB

### 9.1 Breathing Rate Envelop Detection

```
%Author:  Mastan Singh Kalsi
%Date:    April 2009
%Purpose: Breathing Rate Envelope Detection
close all;
load combined.txt

x=combined(:,2);%EXTRACT DATA FROM THE SECOND COLUMN
from=600;
to=3000;
y=x(from:to);

samplePeriod=27.03e-3; %SAMPLING TIME OF SERIAL TRANSMISSION
BRFFT=fft(y); %TAKE THE FOURIER TRANSFORM
N=length(BRFFT);
f=(1/samplePeriod)*(0:(N-1))/N;

BRFFT(f(:)>0.35)=0;%ATTENUATE ALL SIGNALS ABOVE 0.35 Hz
Bir=real(ifft(BRFFT));

figure; %PLOT THE DATA IN GRAPHICAL FORM
plot(1:length(x(from:to)),x(from:to),1:length(Bir),Bir);
```

### 9.2 Peak Detection Algorithm Implementation and the remaining Calculations

```
%Author:  Mastan Singh Kalsi
%Date:    April 2009
%Purpose: Digitally filter the data, implement peak detection, calculate
%         the physiologic health factors along with the correlation
%         coefficients.
close all;
clc;
clear all;
load Mastan_finger.txt %INPUT DATA
output = Mastan_finger;
load IR_Brachial.txt
Broutput=IR_Brachial;
from=14400; %SELECT A RANGE OF DATA TO WORK WITH
to=15000;
figure; %PLOT THE RAW DATA
plot((1:length(output(from:to))),output(from:to));
hold on;
plot((1:length(Broutput(from:to))),Broutput(from:to));
hold off
```

```

xlabel('Sampled Points');
ylabel('Voltage (mV)');
title('Finger PPG (top), Brachial PPG (bottom)');

N=2048;
samplePeriod=27.03e-3; %SAMPLING PERIOD DUE TO SERIAL TRANSMISSION
f=(1/samplePeriod)*(0:(N-1))/N;

IRFFT=fft(output(from:to),N);%FOURIER TRANSFORM
breFFT=fft(output(from:to),N);
IRFFT(200:length(IRFFT))=0;
BIRFFT(200:length(breFFT))=0;
IR=real(ifft(IRFFT));
IR=IR(1:400);
Bir=real(ifft(BreFFT));
Bir=Bir(1:400);

figure %PLOT THE CLEANED SIGNALS
plot((1:400),IR(1:400));
title('IR');
figure
plot((1:400),Bir(1:400));
title('Brachial');

ac=1;%PEAK DETECTION ALGORITHM
irc=1;
peak=0;
peaki=0;
for i=1:400
    if (IR(i)>1050)
        pts(ac)=IR(i);
        if(ac>=3)
            if(pts(ac-2)<pts(ac-1))&&(pts(ac)<pts(ac-1))
                peak=peak+1;
                peakpts(peak)=i;
            end
        end
        ac=ac+1;
    end
    if (Bir(i)>800)
        ptsi(irc)=Bir(i);
        if(irc>=3)
            if(ptsi(irc-2)<ptsi(irc-1))&&(ptsi(irc)<ptsi(irc-1))
                peaki=peaki+1;
                peakptsi(peaki)=i;
            end
        end
        irc=irc+1;
    end
end
peak
peak=peak-1;
scorr=8.67; %CORRELATION COEFFICIENTS
dcorr=11.26;
sdcorr=4.21;
SBP(peak)=zeros;

```

```

DBP(peak)=zeros;
dcorrelated(peak)=zeros;
dactual(peak)=zeros;
IHR(peak)=zeros;

if peak>28
    peak=28;
end
for j=1:peak
    ptt(j)=peakpts(j+1)-peakptsi(j);
    IHR(j)= (1/((peakpts(j+1)-peakpts(j))*samplePeriod))*60;

    Y=min(IR(peakpts(j):peakpts(j+1)));
    ph(j)=IR(peakpts(j+1))-Y;
    SBP(j)=IR(peakpts(j+1))/scorr;
    DBP(j)=Y/dcorr;
    dcorrelated(j)=ph(j)/sdcorr;
    dactual(j)=SBP(j)-DBP(j);
    if (abs(dcorrelated(j)-dactual(j))>5)
        SBP(j)=SBP(j-1);
        DBP(j)=DBP(j-1);
    end
end
ph
ptt
SBP
DBP
dcorrelated-dactual
IHR
for j=1:peak-1 %STANDARD DEVIATION FOR HRV
    HRV(j)=std(IHR(j:j+1));
end
HRV %OUTPUT DATA
figure
plot(ph);
title('pulse height');
figure
plot(ptt);
title('pulse transit time');
figure
plot(SBP)
axis([0 12 80 160]);
title('sbp');

figure
plot(DBP)
axis([0 12 40 100]);
title('dbp');

figure
plot(IHR)
title('ihr');
figure
plot(HRV)
axis([1 12 1 25]);
title('hrv');

```

## 10 REFERENCES

- [1] Canadian Hypertension Society, *Blood Pressure Information*, [online] 2008, <<http://www.hypertension.ca/>> (Accessed: October 4<sup>th</sup>, 2008).
- [2] W. S. Johnston and Y. Mendelson, "Extracting breathing rate information from a wearable reflectance pulse oximeter sensor," *Engineering in Medicine and Biology Society, 2004. IEMBS '04. 26th Annual International Conference of the IEEE*, vol. 2, pp. 5388-5391, 2004.
- [3] W. Johnston and Y. Mendelson, "Extracting heart rate variability from a wearable reflectance pulse oximeter," *Bioengineering Conference, 2005. Proceedings of the IEEE 31st Annual Northeast*, pp. 157-158, 2005.
- [4] H. Coni and N. Coni, *Blood Pressure – all you need to know*, Illinois: Royal Society of Medicine Press Ltd, 2003, pp. 2.
- [5] Sujay Deb, C. Nanda, D. Goswami, J. Mukhopadhyay and S. Chakrabarti, "Cuff-Less Estimation of Blood Pressure Using Pulse Transit Time and Pre-ejection Period," *Convergence Information Technology, 2007. International Conference on*, pp. 941-944, 2007.
- [6] I. Rapoport and A. J. Cousin, "A Pilot Clinical PEP Monitor," *Biomedical Engineering, IEEE Transactions on*, vol. BME-26, pp. 345-349, 1979.
- [7] X. F. Teng and Y. T. Zhang, "Continuous and noninvasive estimation of arterial blood pressure using a photoplethysmographic approach," *Engineering in Medicine and Biology Society, 2003. Proceedings of the 25th Annual International Conference of the IEEE*, vol. 4, pp. 3153-3156 Vol.4, 2003.
- [8] Digikey, *Photodiode Parts Information*, [online] 2008, <<http://parts.digikey.com/1/parts/1540920-photodiode-t1-3-4-sfh-203-p.html/>> (Accessed: October 14<sup>th</sup>, 2008).
- [9] H. Coni and N. Coni, *Blood Pressure – all you need to know*, Illinois: Royal Society of Medicine Press Ltd, 2003, pp. 6.
- [10] R. S. Khandpur, *Handbook of Biomedical Instrumentation*, 2<sup>nd</sup> ed. New Delhi: Tata McGraw-Hill Publishing Company Limited, 2003, pp. 113.

- [11] R. C. Jaeger and T. N. Blaclock, *Microelectronic Circuit Design*, 2<sup>nd</sup> ed. New York: The McGraw Hill Companies, 2004, pp. 157-158.
- [12] B. H. Timmons and R. Ley, *Behavioural and psychological approaches to breathing disorders*, pp. 36.



## 11 VITAE

NAME: Mastan Singh Kalsi

PLACE OF BIRTH: Jagraon, Punjab, India

YEAR OF BIRTH: 1984

SECONDARY EDUCATION: Turner Fenton Secondary School  
(1998 – 2003)

UNDERGRADUATE EDUCATION: Kinesiology and Health Sciences  
(2003 – 2004)  
Electrical and Biomedical Engineering  
(2004 – 2009)

WORK EXPERIENCE: Internship Position –  
Research In Motion Limited  
(2007 – 2008)

HONOURS AND AWARDS: Queen Elizabeth II Scholarship  
(2003)  
York University Entrance Scholarship  
(2003)  
Kinesiology and Health Sciences  
Faculty Scholarship  
(2003)